The Galt & Kennedy “Dominion” List “A” and My Favourite DA Sources

Roland Kothes

Dominion Radio Astrophysical Observatory
National Research Council
Herzberg Programs of Astronomy & Astrophysics

DRAO, September 21, 2014

The Radio Sky

Haslam et al, 1982

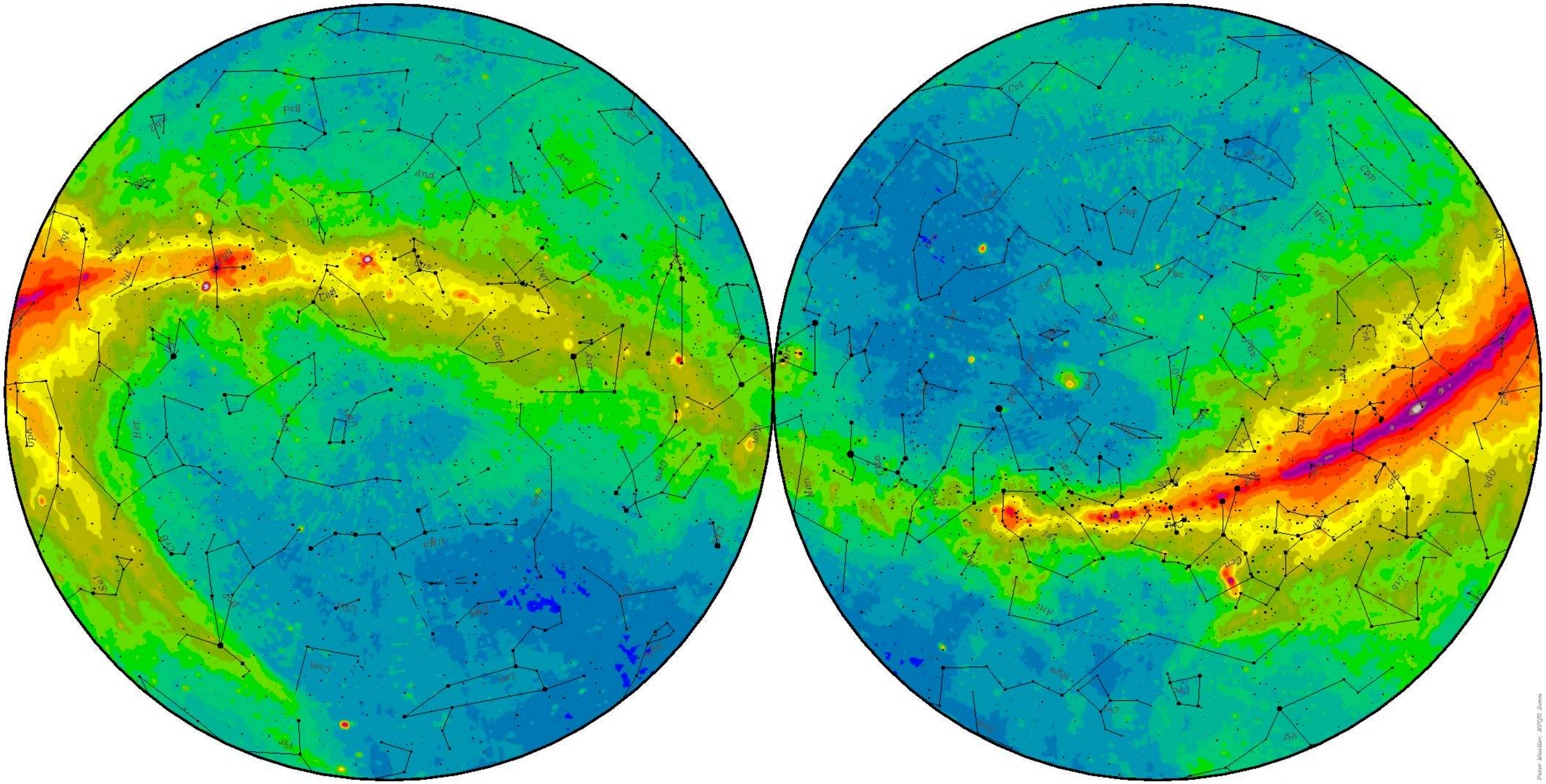

ⓒPeter Müller, Max Planck Institut für Radioastronomie.

The DRAO 26m John Galt Telescope

The 1420 MHz Drift-Scan Sky Survey

- Drift-scan survey with the John Galt Telescope near 1420 MHz
- Resolution: $\approx 36'$
- Observations began in July 1963 and continued until July of 1967
- To avoid problems with solar interference the observations were made between sunset and sunrise.
- Drift-scans were obtained every 15’ between declinations -5° and $+70^\circ$.
- Background emission was published in the Masters and PhD thesis of John E.D. Kennedy.

The “Dominion” List “A” Catalogue

last copy ?

CANADA
DEPARTMENT OF ENERGY, MINES AND RESOURCES
DOMINION OBSERVATORIES

CONTRIBUTIONS

from the

Dominion Observatory

OTTAWA

Vol. 4, No. 26

SURVEY OF RADIO SOURCES OBSERVED IN THE CONTINUUM NEAR 1420 MHz, DECLINATIONS -5° TO +70°

BY

J.A. Galt and J.E.D. Kennedy

Reprinted from

THE ASTRONOMICAL JOURNAL
73, 135 (1968)

The “Dominion” List “A” Catalogue

last copy ?

CANADA
DEPARTMENT OF ENERGY, MINES AND RESOURCES
DOMINION OBSERVATORIES

CONTRIBUTIONS
from the
Dominion Observatory
OTTAWA

Vol. 4, No. 26

SURVEY OF RADIO SOURCES OBSERVED IN THE CONTINUUM NEAR 1420 MHz, DECLINATIONS -5° TO +70°
BY
J.A. Galt and J.E.D. Kennedy

Reprinted from
THE ASTRONOMICAL JOURNAL
73, 135 (1968)

Survey of Radio Sources Observed in the Continuum near 1420 MHz, Declinations −5° to +70°

J. A. Galt and J. E. D. Kennedy
Dominion Radio Astrophysical Observatory, Penticton, B. C., Canada
(Received 12 January 1968)

A catalogue of 615 radio sources is presented. These have been observed with a 36′ beam near 1420 MHz during a drift-scan survey of the sky. The survey is believed complete to a flux level of 2×10^{-26} W $m^{-2}Hz^{-1}$. The slope of the log N/log S plot for sources away from the galactic plane is -1.88 ± 0.07. There appears to be no evidence for a change of slope with frequency. A study has been made of the distribution of spectral indices for those sources which are common to the present survey and the 4C catalogue. For sources selected at 1420 MHz there is no change in median spectral index with flux density. Fluxes of some of the survey sources have also been observed with a beamwidth of 8′.9 at 3200 MHz.

INTRODUCTION

A SURVEY of the continuum radiation near 1420 MHz has been made using a 25.6-m parabolic antenna. Drift scans were obtained every quarter degree or approximately every half beamwidth between declinations −5° and +70°.

The survey was undertaken to search for new sources that had not been found in previous lower frequency surveys and to provide spectral data on those sources already known. Many of the sources have also been observed at 3200 MHz; a few of these appear to have spectra rising rapidly at high frequencies.

APPARATUS

The telescope and radiometer have been described by Locke, Galt, and Costain (1965). A Dicke switch compares the noise power received by a horn at the focus of the paraboloid to the power from a matched termination at 90°K. Extra noise power is injected into the antenna side of the switch to balance the system in the absence of strong sources. Linear polarization is used with the E-vector parallel to the lines of declination. The first stage of the receiver is an electron beam parametric amplifier. Its pump frequency was chosen so that the "signal" and "idler" bands fall symmetrically on either side of the hydrogen-line frequency. Each band is 6 MHz wide, the actual observing frequencies being 1413.4 to 1419.4 and 1421.4 to 1427.4 MHz. Thus the receiver accepts two bands simultaneously, the mean frequency being 1420.4 MHz. The over-all noise temperature, including the extra noise required for balancing, was ≈270°K. Receiver gain was held constant with an automatic gain control system sensing only the power from the comparison resistor side of the switching cycle. The receiver showed no significant departure from linearity over the 1000 to 1 range of intensity encountered.

Observations began in July 1963 and continued until July 1967. To avoid problems of solar interference all observations were made between sunset and sunrise. Most scans were taken with the telescope on the meridian.

3200 MHz OBSERVATIONS

Measurements were made at the Algonquin Radio Observatory (ARO) of the National Research Council using the precision 46-m paraboloid. The radiometer in this case was a tunnel diode receiver with a bandwidth of 600 MHz. A Dicke switching system was used with a stable room-temperature comparison resistor. Analogue output only was employed with simultaneous output bandwidths of 0.08 and 0.025 Hz. Observations were made by scanning in right ascension or declination and by "on–off" measurements. The beamwidth at this frequency was 8′.9.

DATA REDUCTION

The output of the 1420-MHz radiometer was fed to a linear integrator which averaged the signals for 30 sidereal seconds. The resultant voltages were read by a digital voltmeter and automatically punched on cards. The cards were than processed with a digital computer to reduce deflections to a common intensity scale by comparison with a calibration that had been applied at the beginning and end of each observing period. The data were convolved with a declination-dependent function derived from the beam shape to remove high-frequency fluctuations that could not have been generated by the antenna beam while scanning the sky. The computer finally produced a series of plots of temperature vs right ascension. These were plotted to a uniform scale with adjacent traces displaced in declination as shown in Fig. 1. With this display, strong sources appeared on at least three adjacent traces while fainter sources could be detected on at least two.

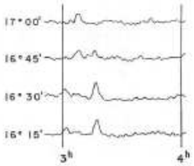

Fig. 1. A portion of the computer-generated plot showing, left to right, 3C76.1, 3C79, and CTA 21. In general, sources are not as closely spaced as this illustration would suggest.

The "Dominion" List "A" Catalogue

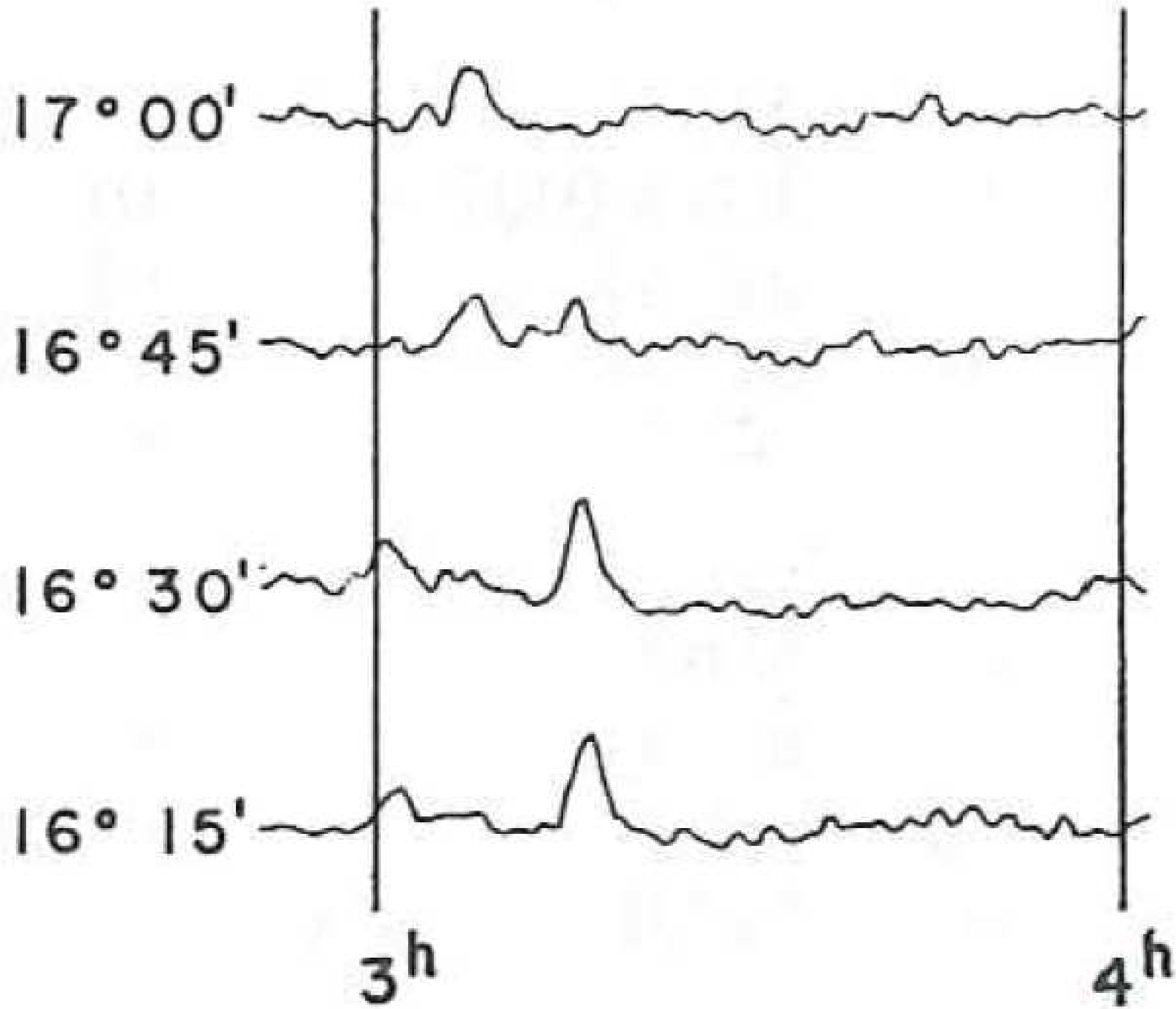

The “Dominion” List “A” Catalogue

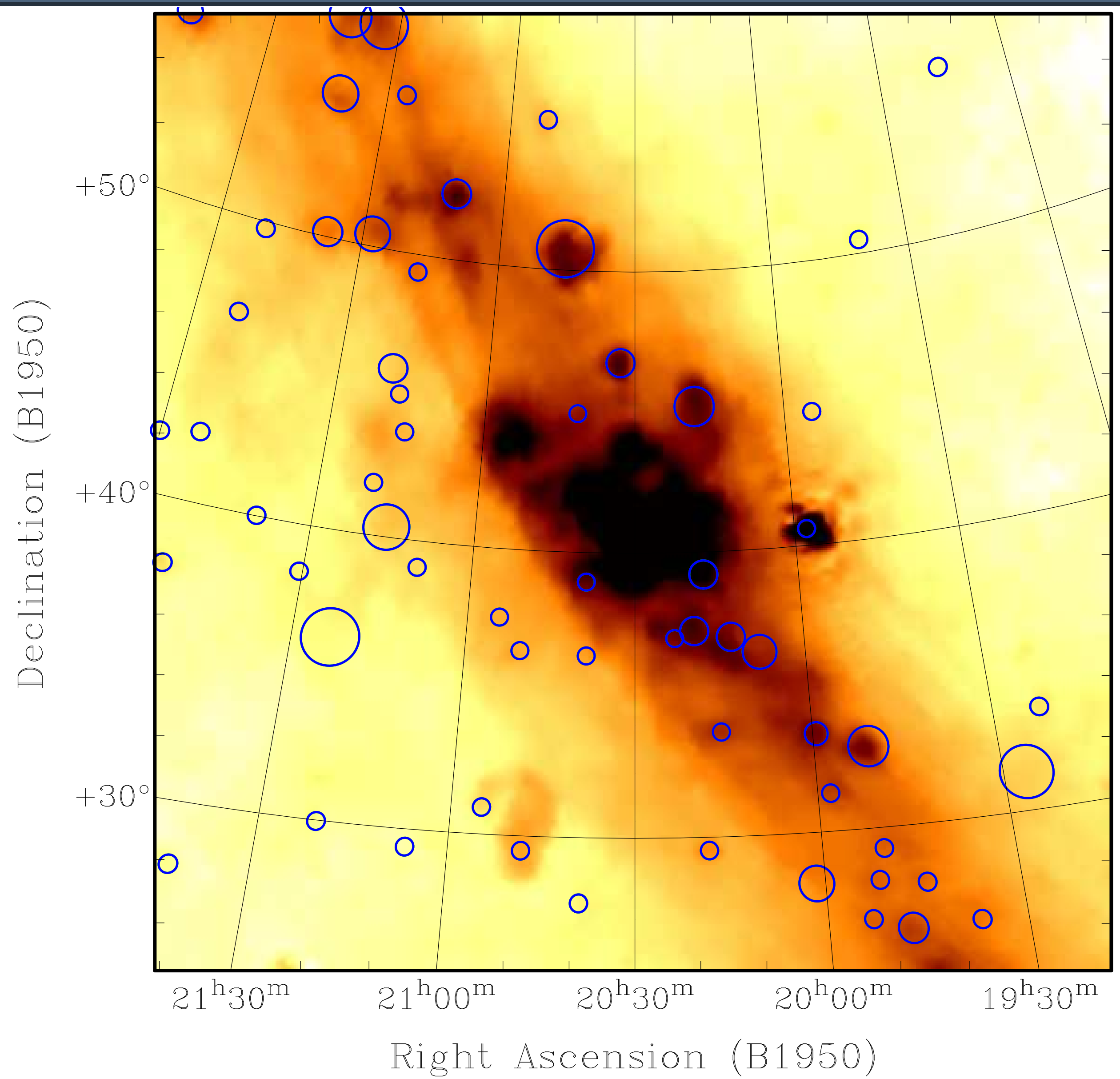

Map: Reich, 1982 (Stockert 21cm Survey)

The “Dominion” List “A” Catalogue

- 615 catalogued radio sources
- 81 new radio sources
- SNRs, HII region, Quasars, Galaxies, etc.
- believed to be complete down to a flux level of $2 \times 10^{-26}\,\mathrm{W\,m^{-2}\,Hz^{-1}}$
- some sources were also observed at 3200 MHz with the Algonquin Radio Observatory

The Algonquin Radio Observatory

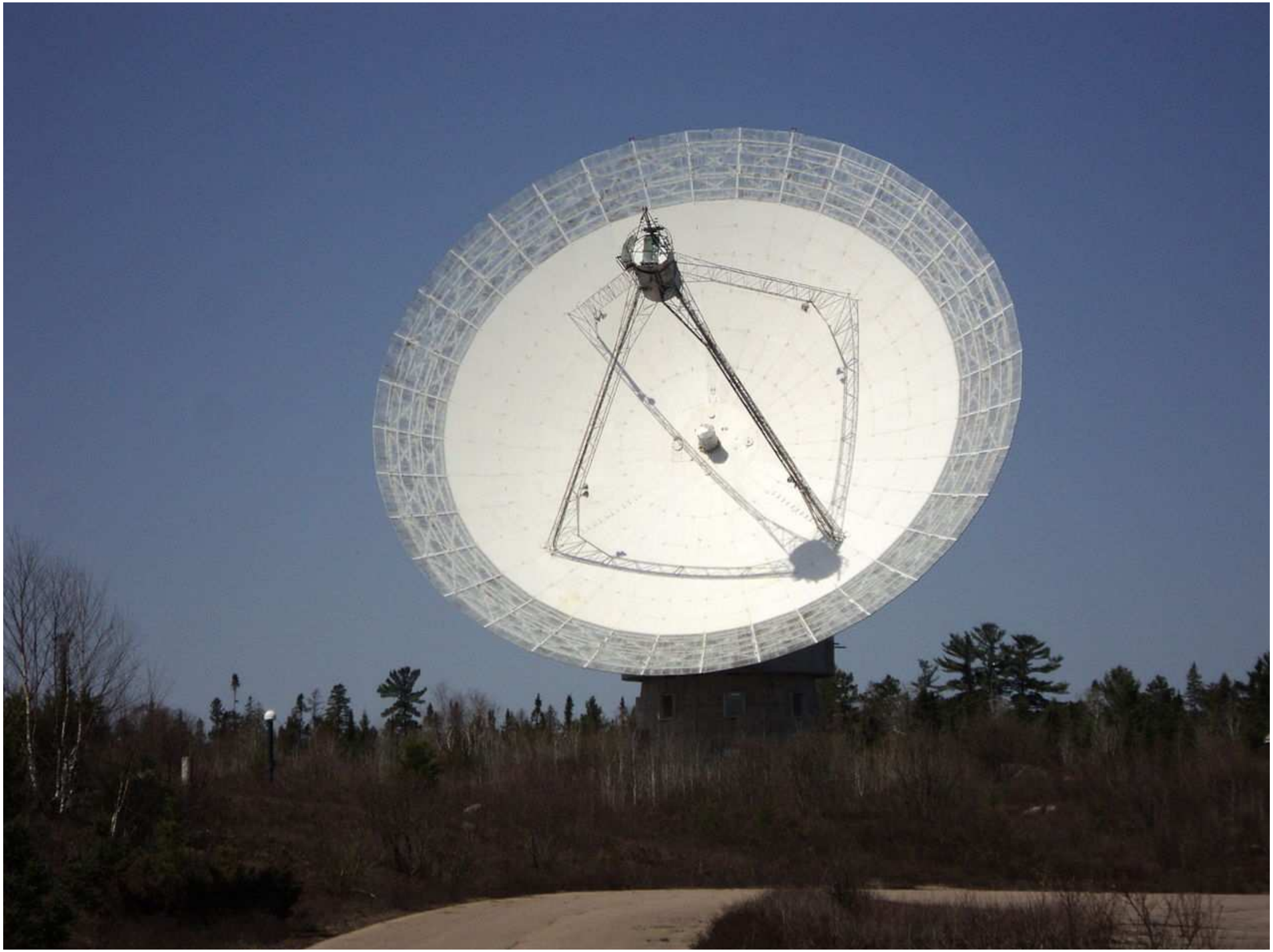

DA 530

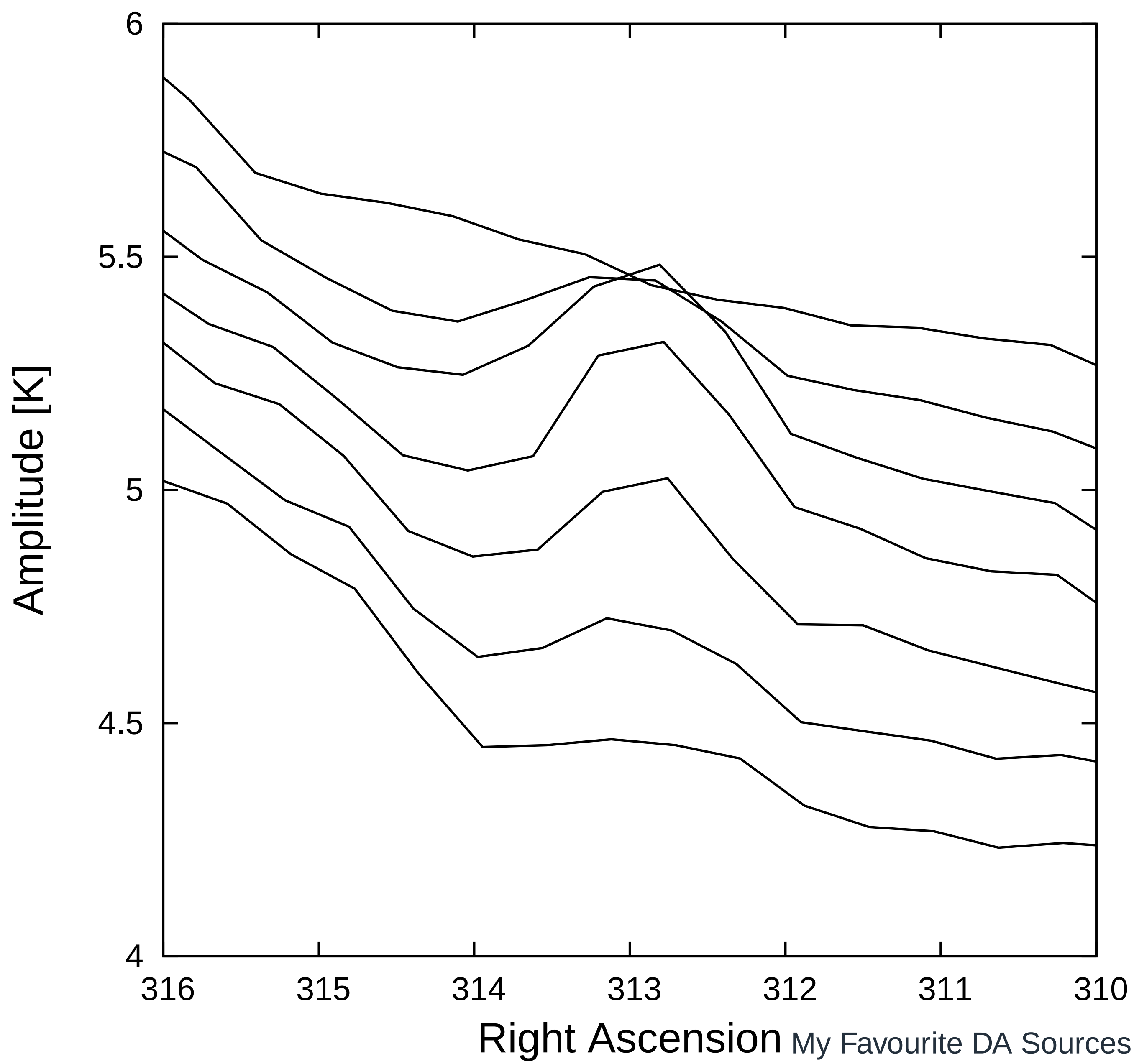
6
5.5
5
4.5
4
316
315
314
313
312
311
310
Amplitude [K]
Right Ascension

SNR DA 530 with the DRAO ST

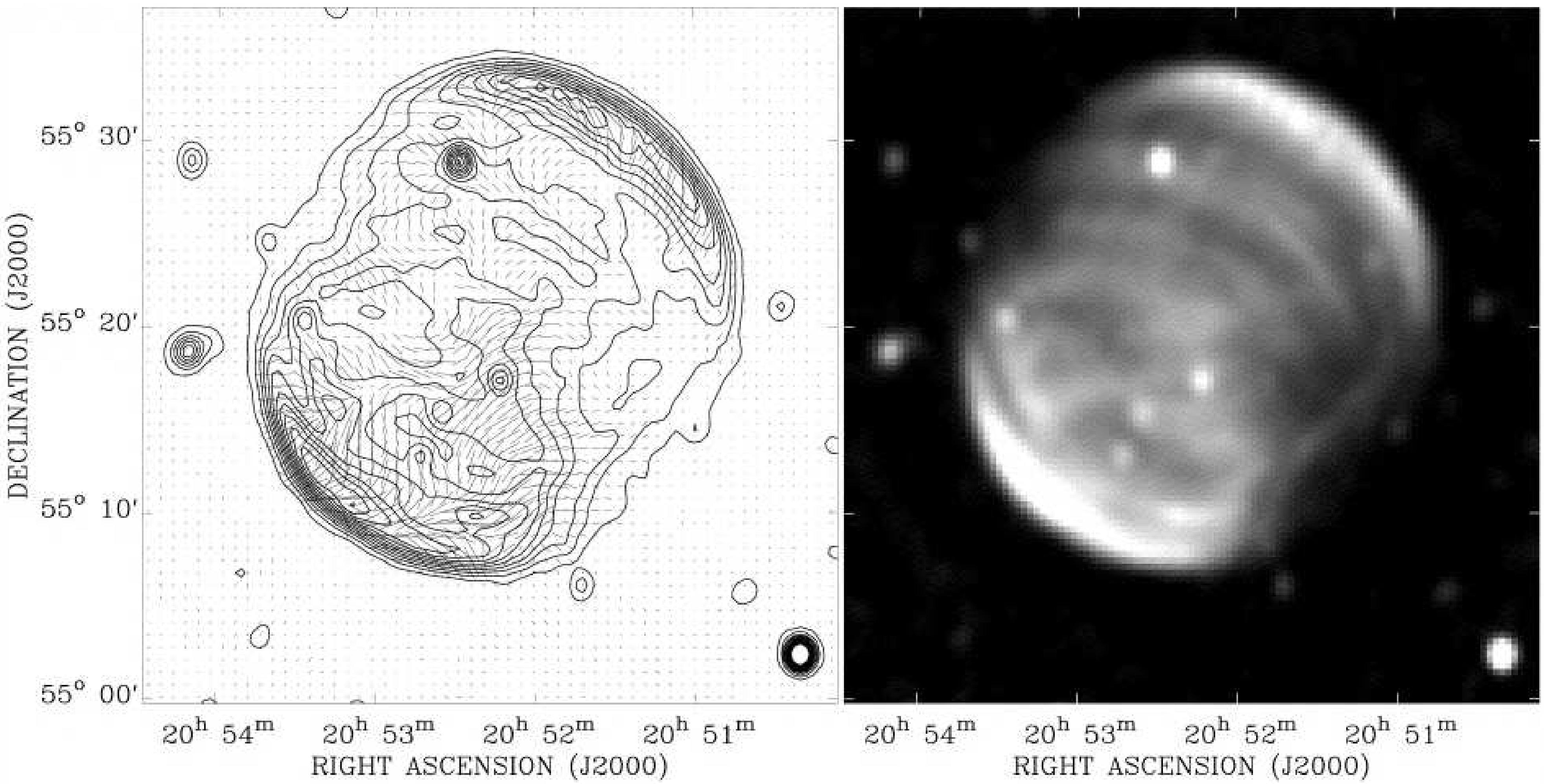

Landecker et al., 2000

Radio Continuum Spectrum DA 530

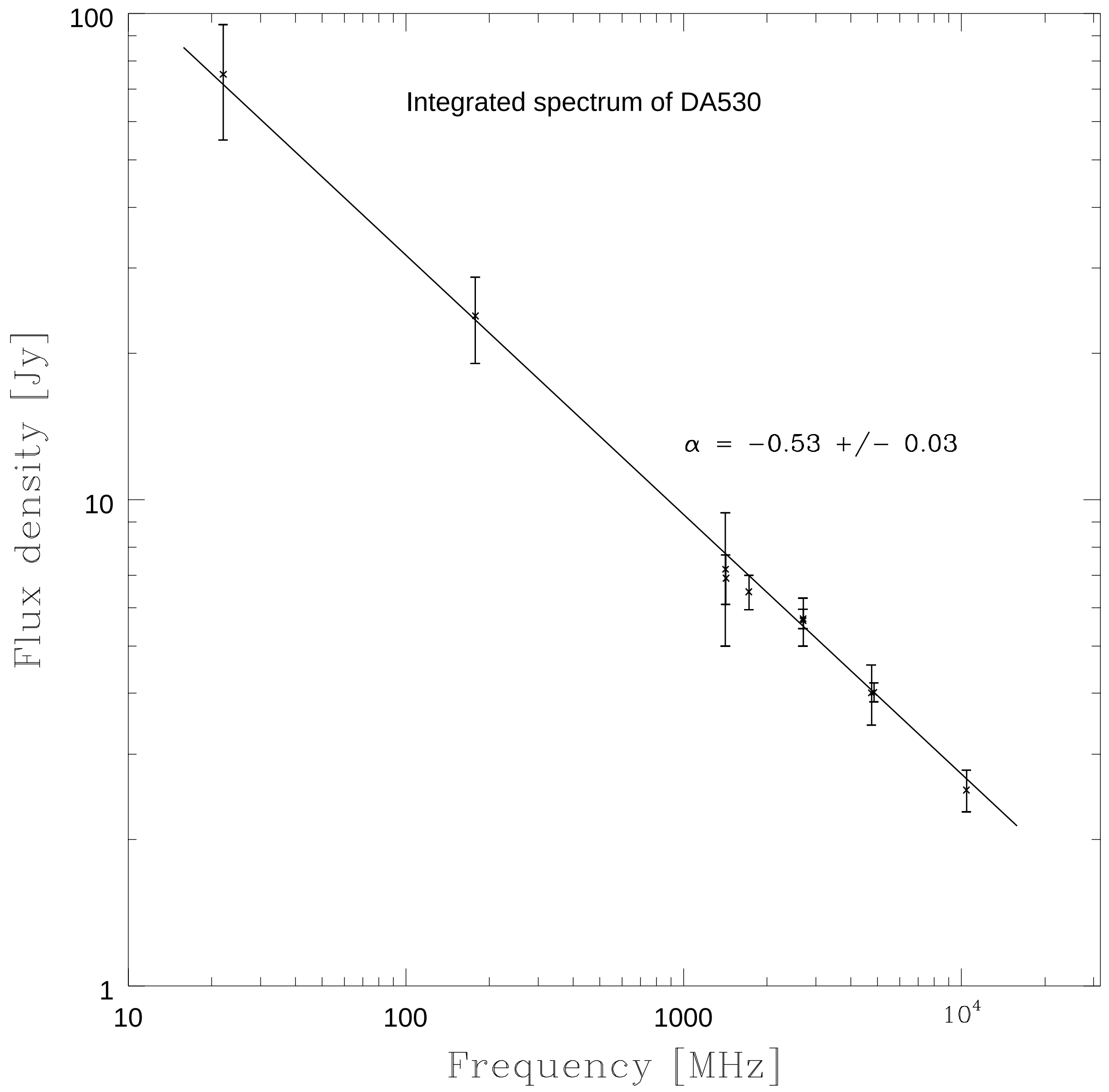

SNR DA 530 with the DRAO ST

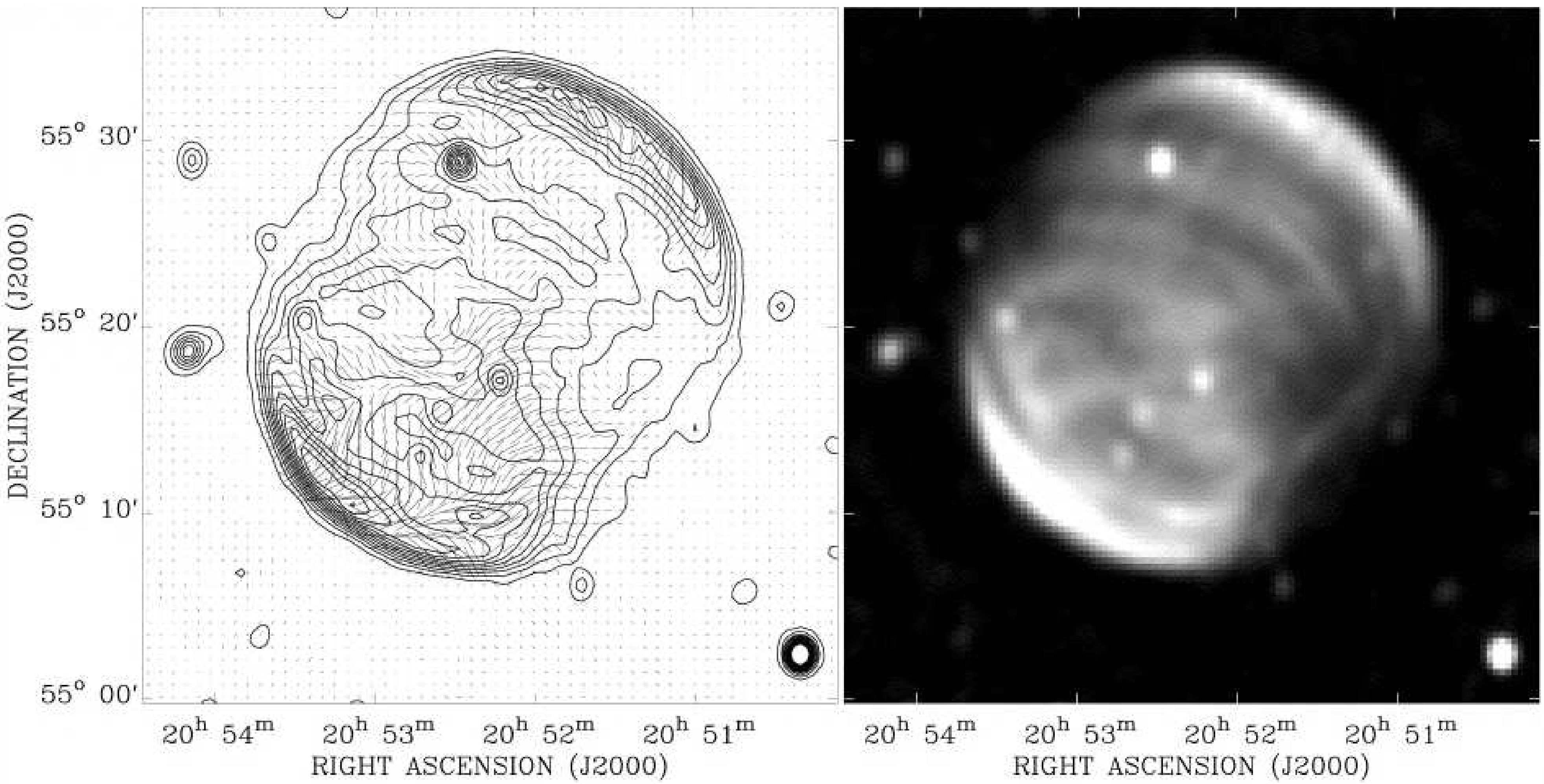

Landecker et al., 2000

DA 530 with Effelsberg

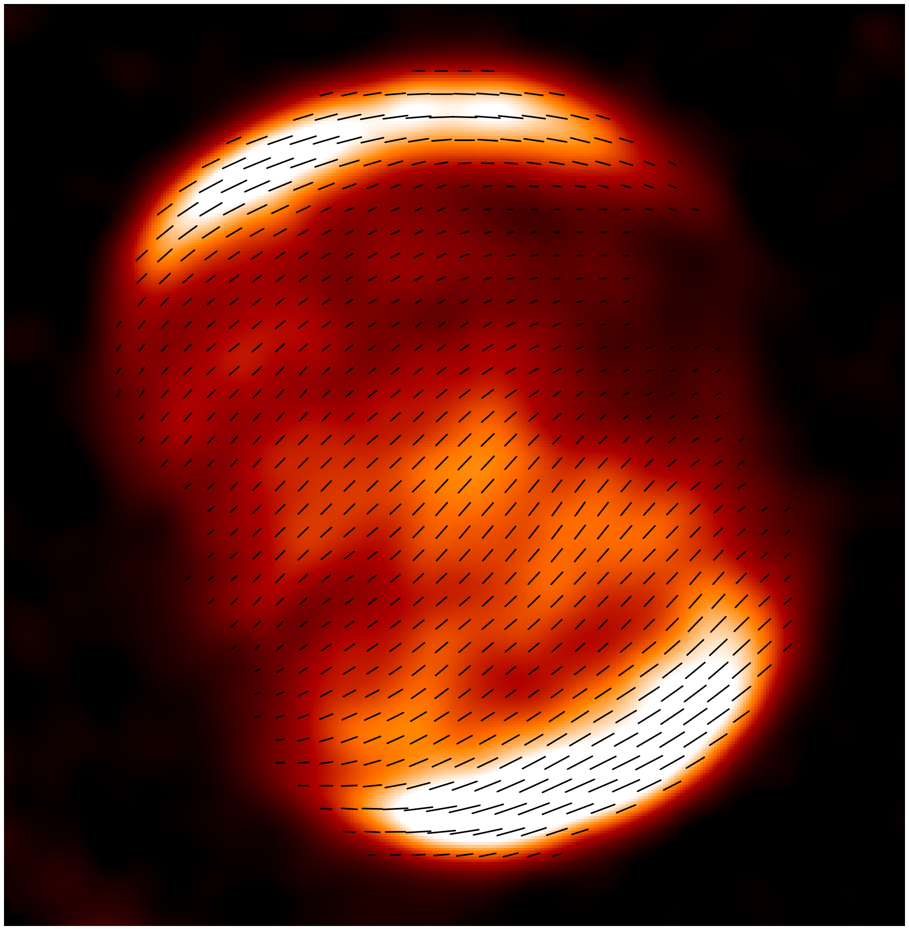

DA 530 at 10.6 GHz (Effbg 100m)
B-vectors are overlaid.

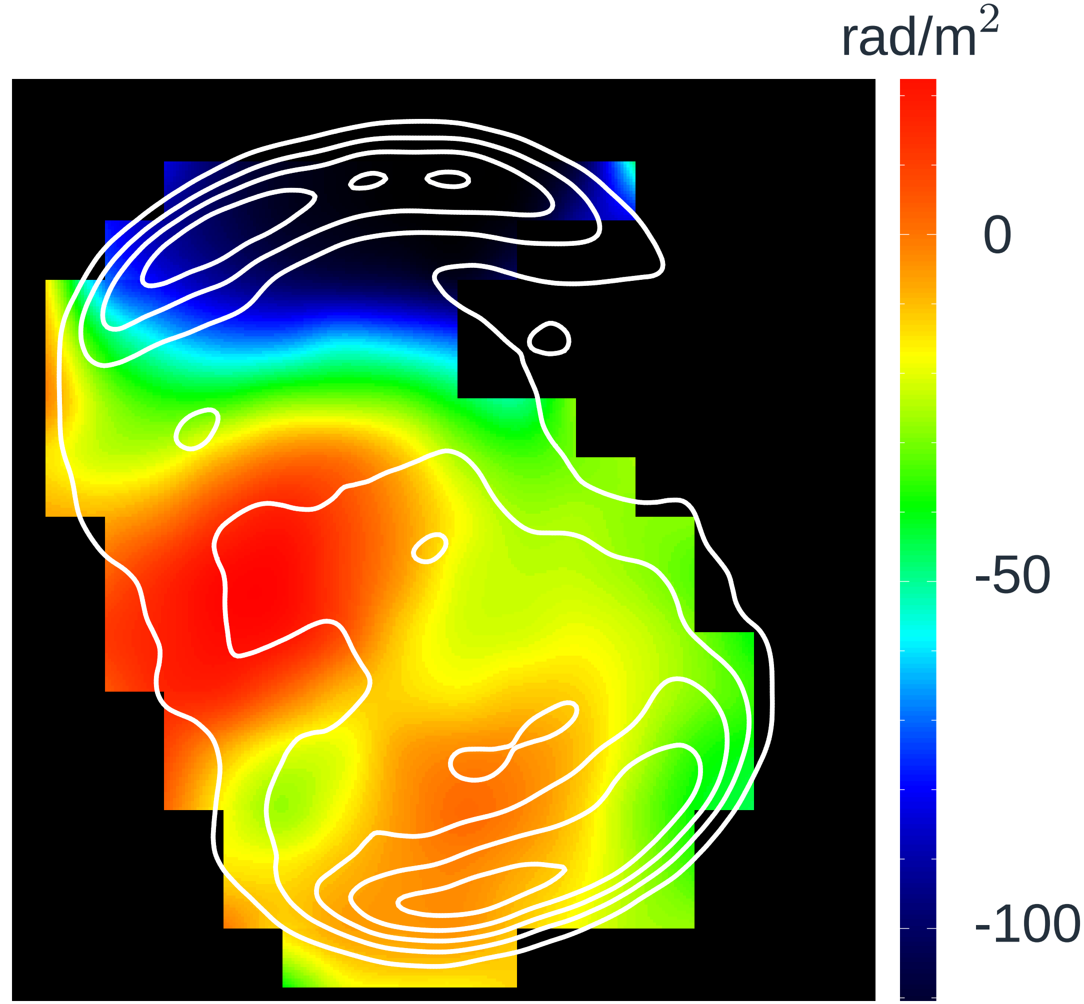

Rotation Measure Map of DA 530

DA 530 the standard shell-type SNR

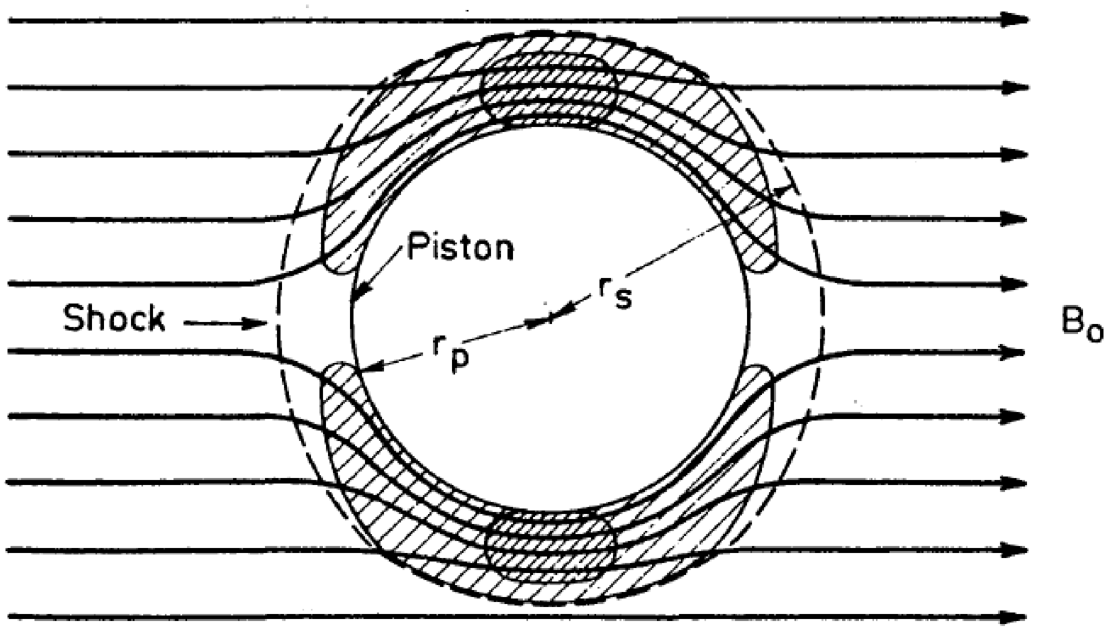

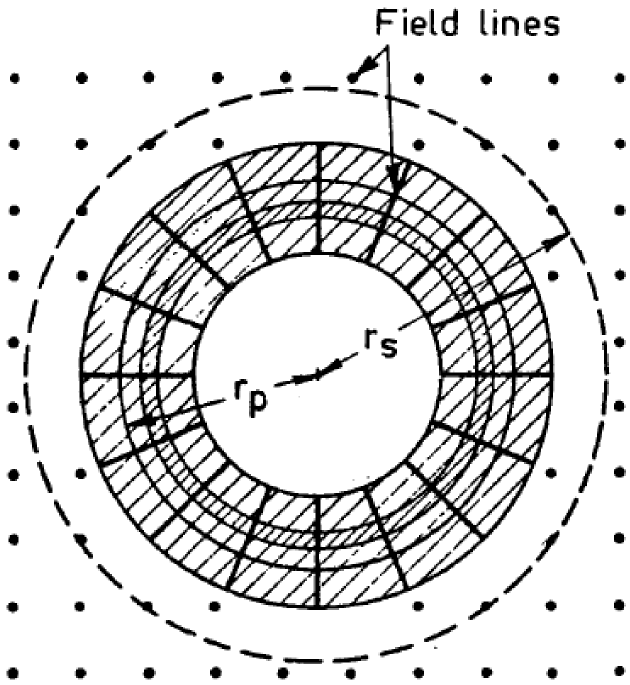

Whiteoak & Gardner, 1968

A Model of a Mature SNR

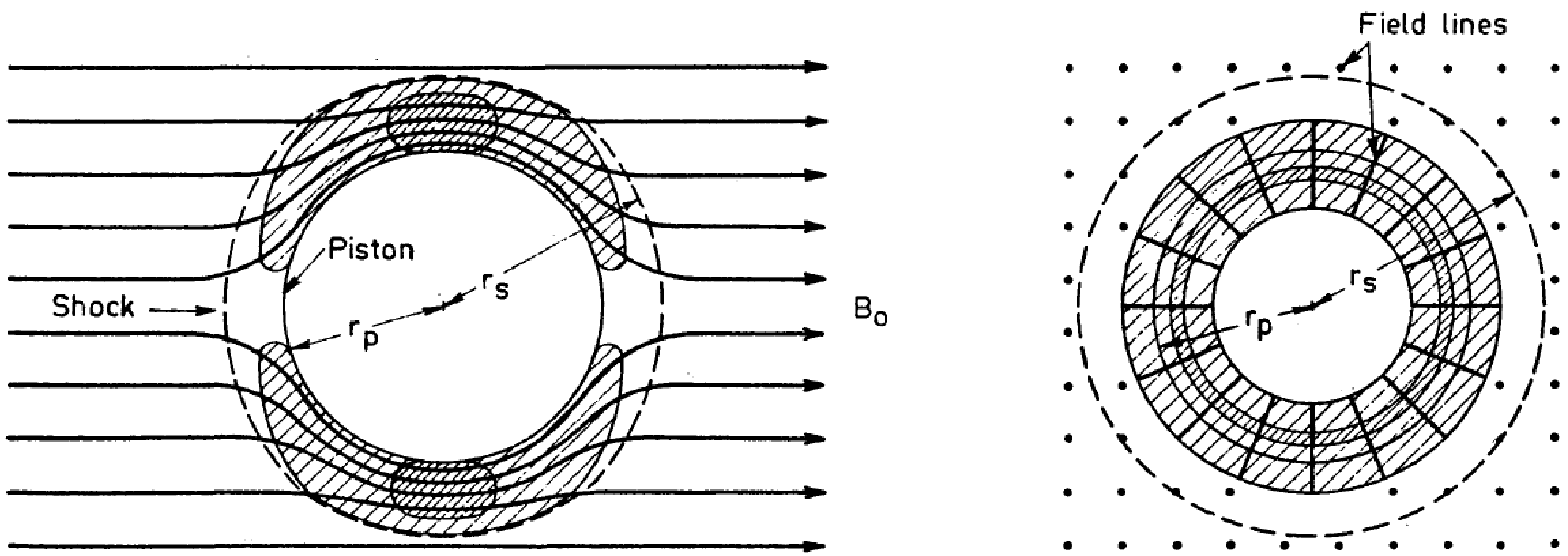

I assume:

- mature SNR $\Rightarrow$ dominated by environment
- spherical geometry
- constant ambient density n_0 ($= 1\,$cm^{-3})
- homogenous ambient magnetic field $\vec{B}_0$ ($= 5\,\mu$G)

A Model of a Mature SNR

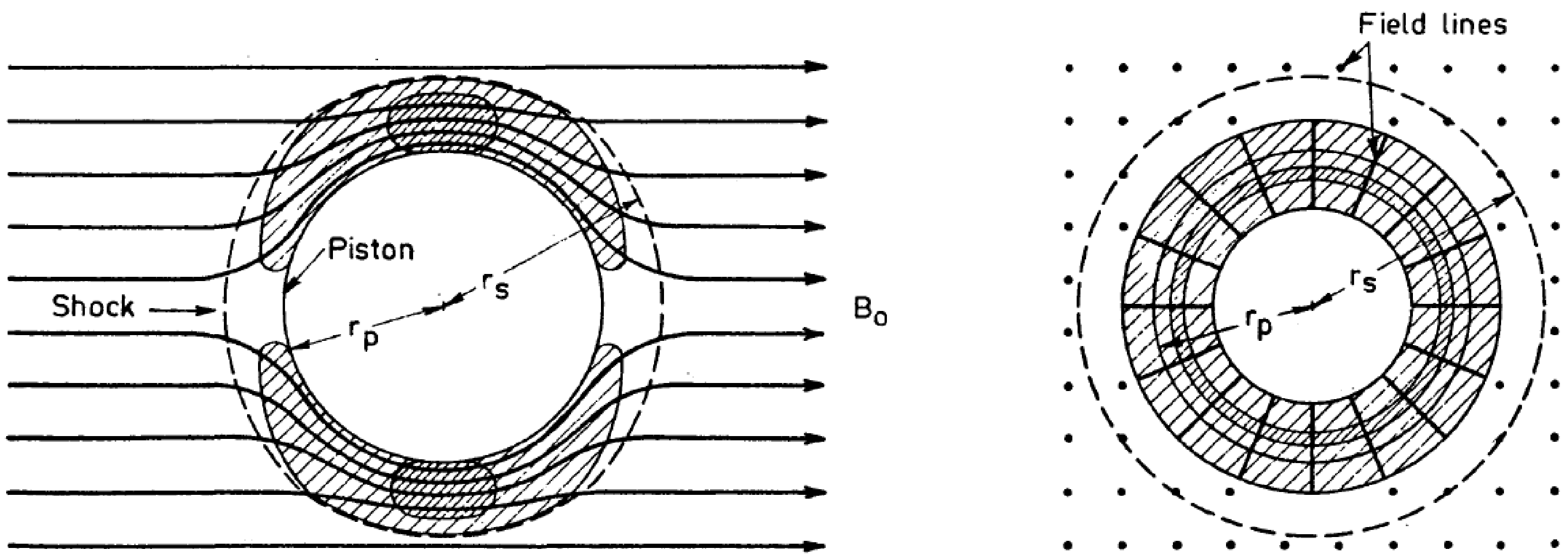

- Θ: angle between plane of the sky and ambient B-field
- $S_\nu = K\, B_\perp^{\frac{1}{2}(\delta+1)} \nu^{-\frac{1}{2}(\delta-1)}, N(E)dE = K\, E^{-\delta} dE$
- $\Delta\phi_\lambda = RM\lambda^2$, $RM = 0.81 \int_l B_\| n_e dl$

Emission Structure of SNRs

Rotation Angle $\Theta = 0^\circ$

Stokes I | PI + B-vectors

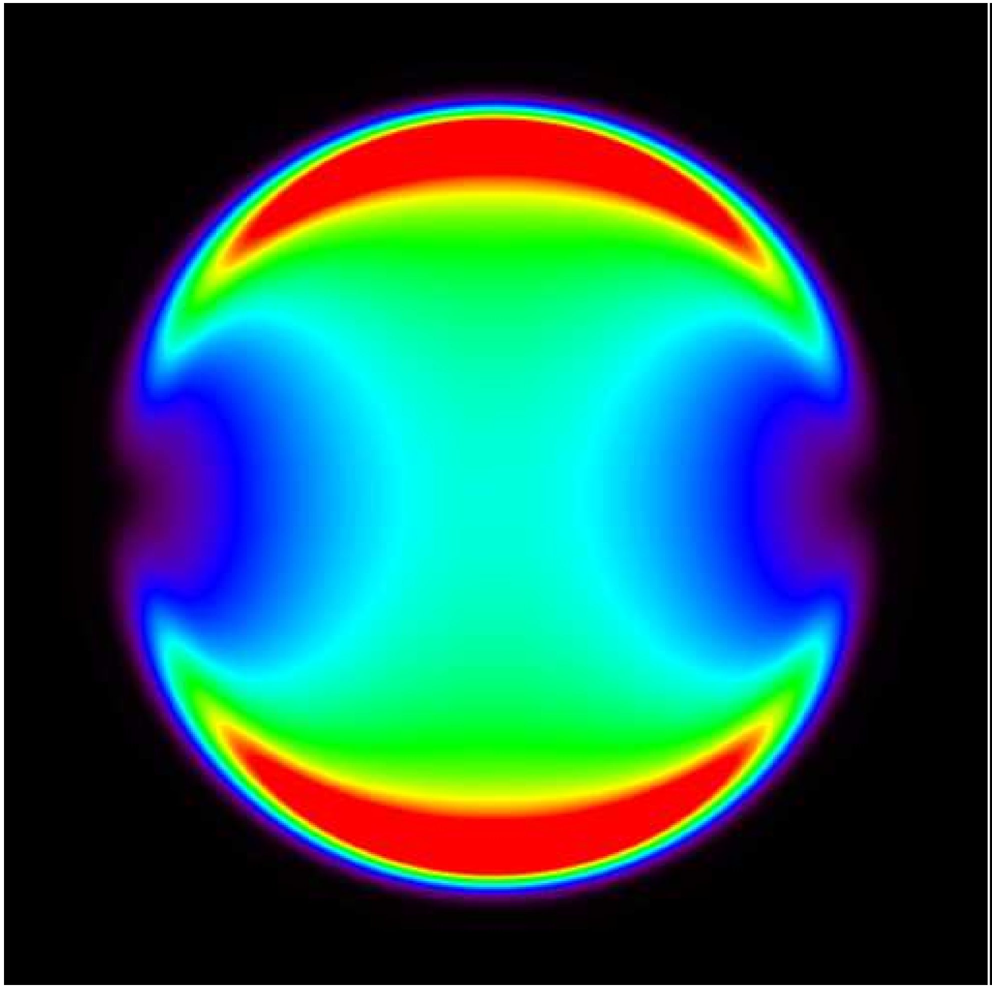

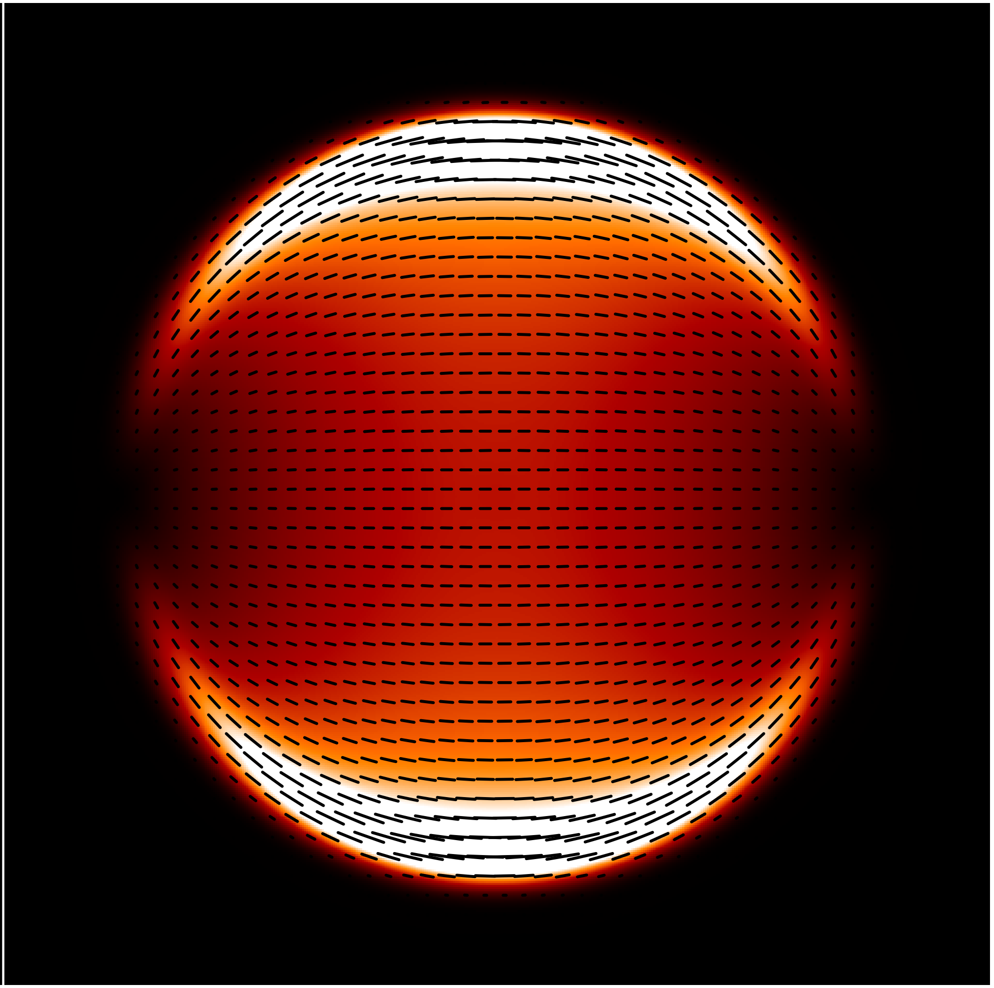

Emission Structure of SNRs

Rotation Angle $\Theta = 15^\circ$

Stokes I

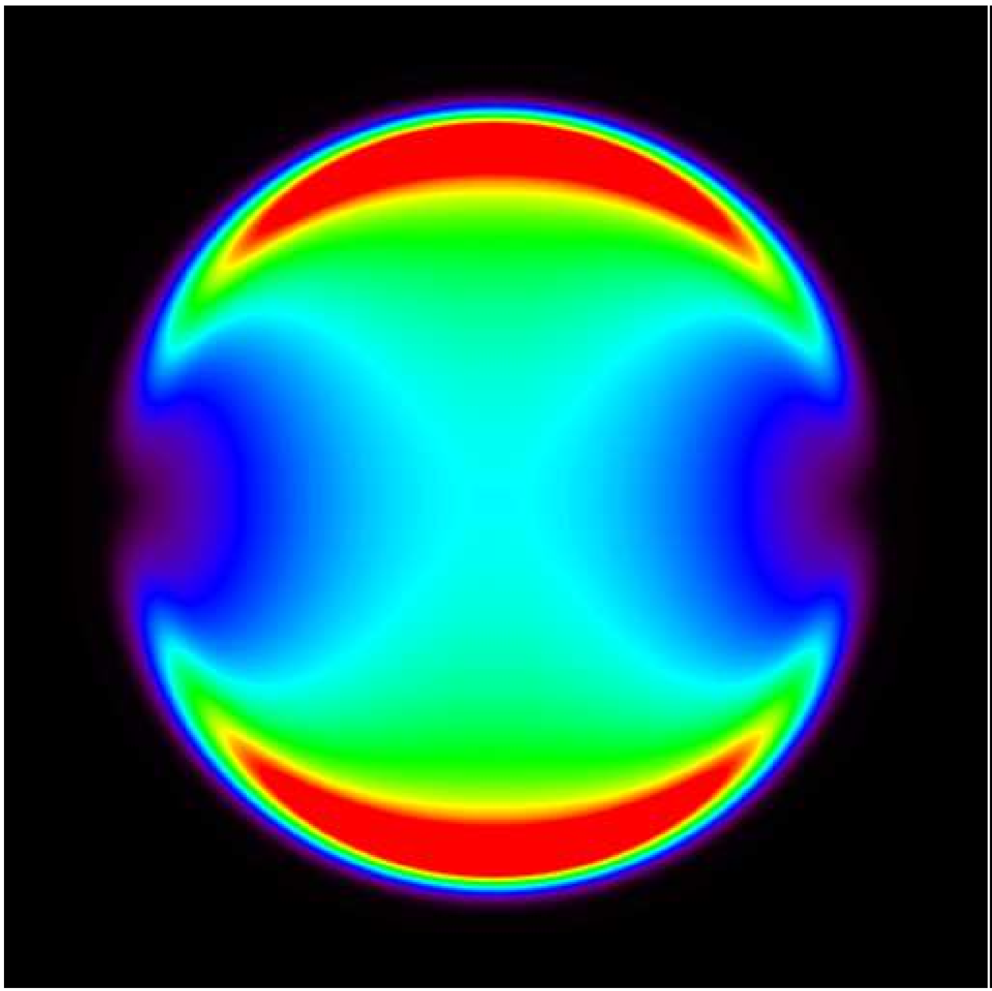

PI + B-vectors

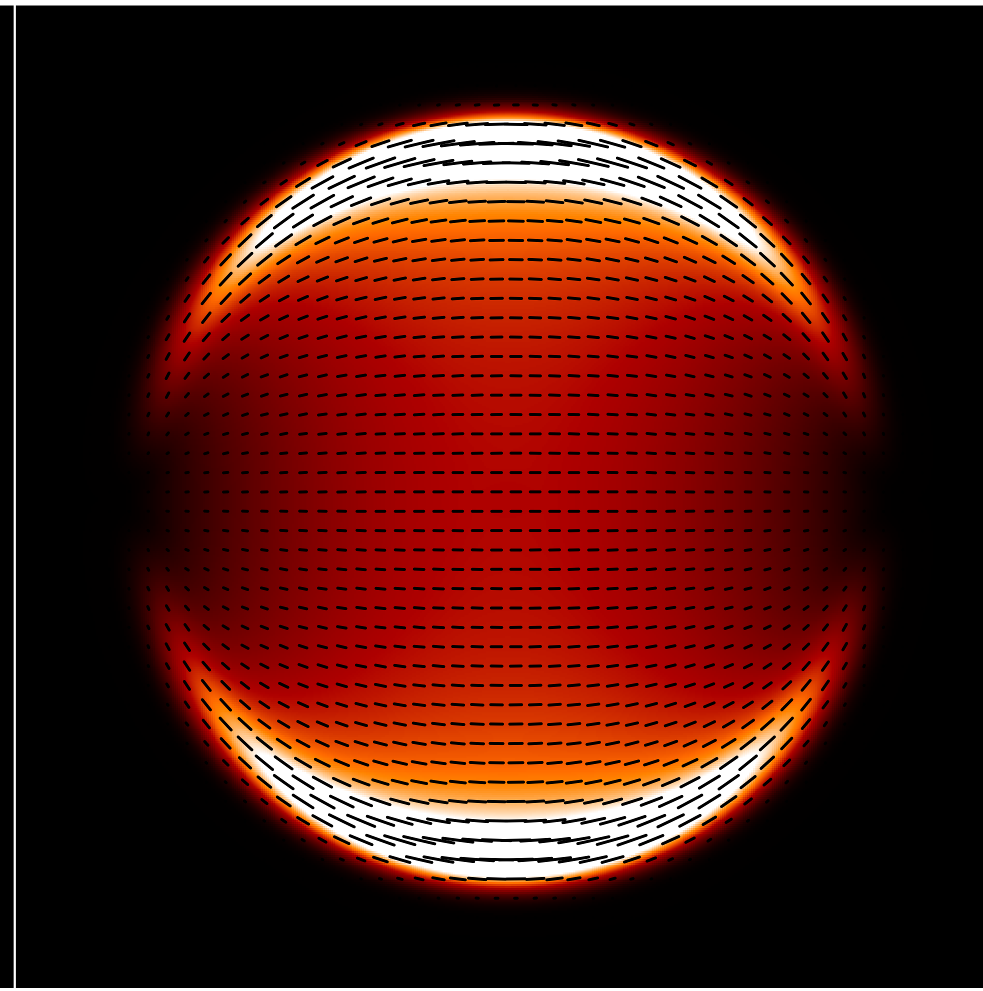

Emission Structure of SNRs

Rotation Angle $\Theta = 30^{\circ}$

Stokes I

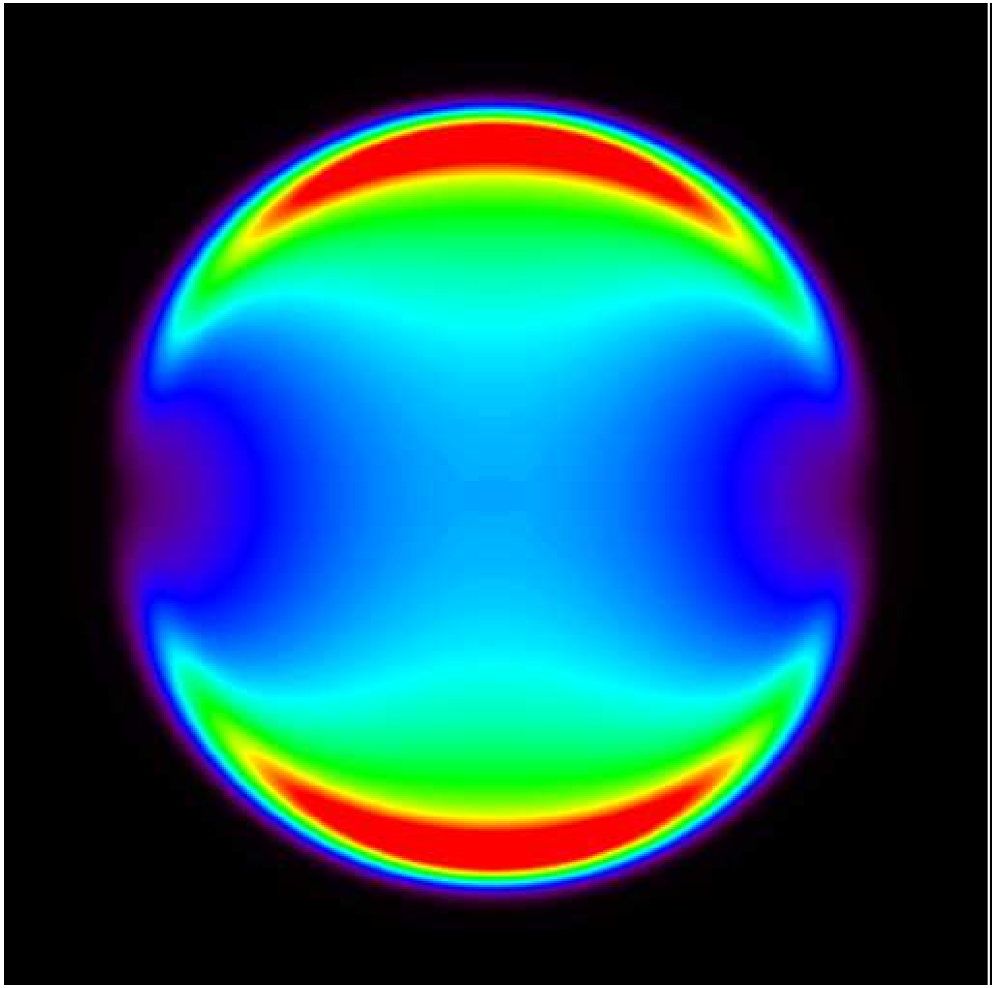

PI + B-vectors

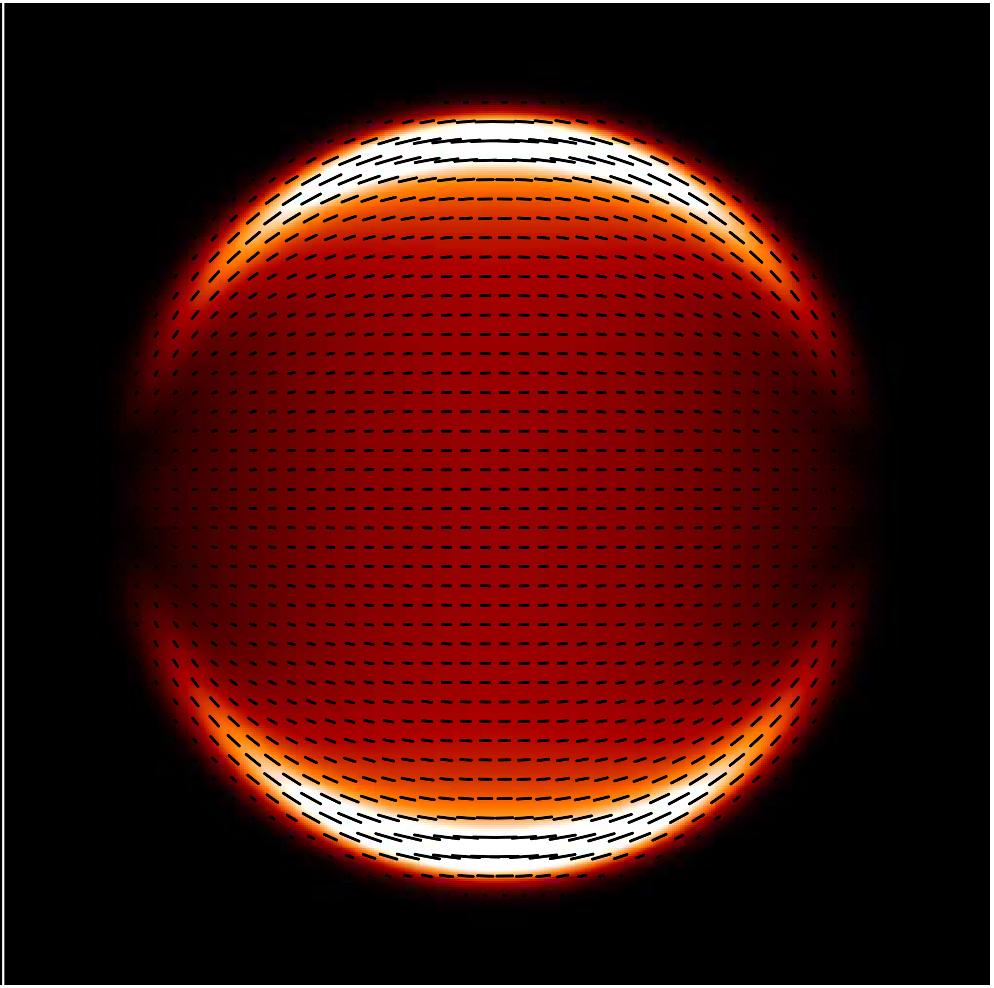

Emission Structure of SNRs

Rotation Angle $\Theta = 45°$

Stokes I	PI + B-vectors
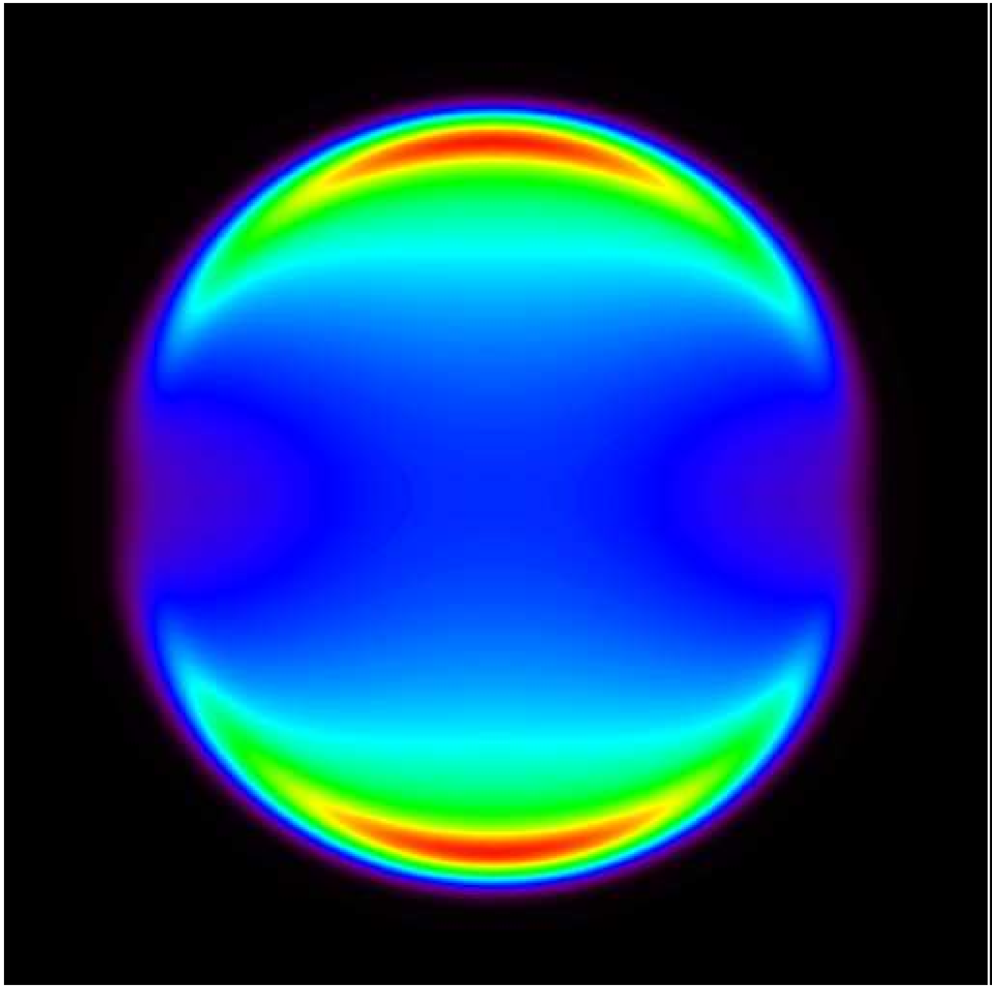	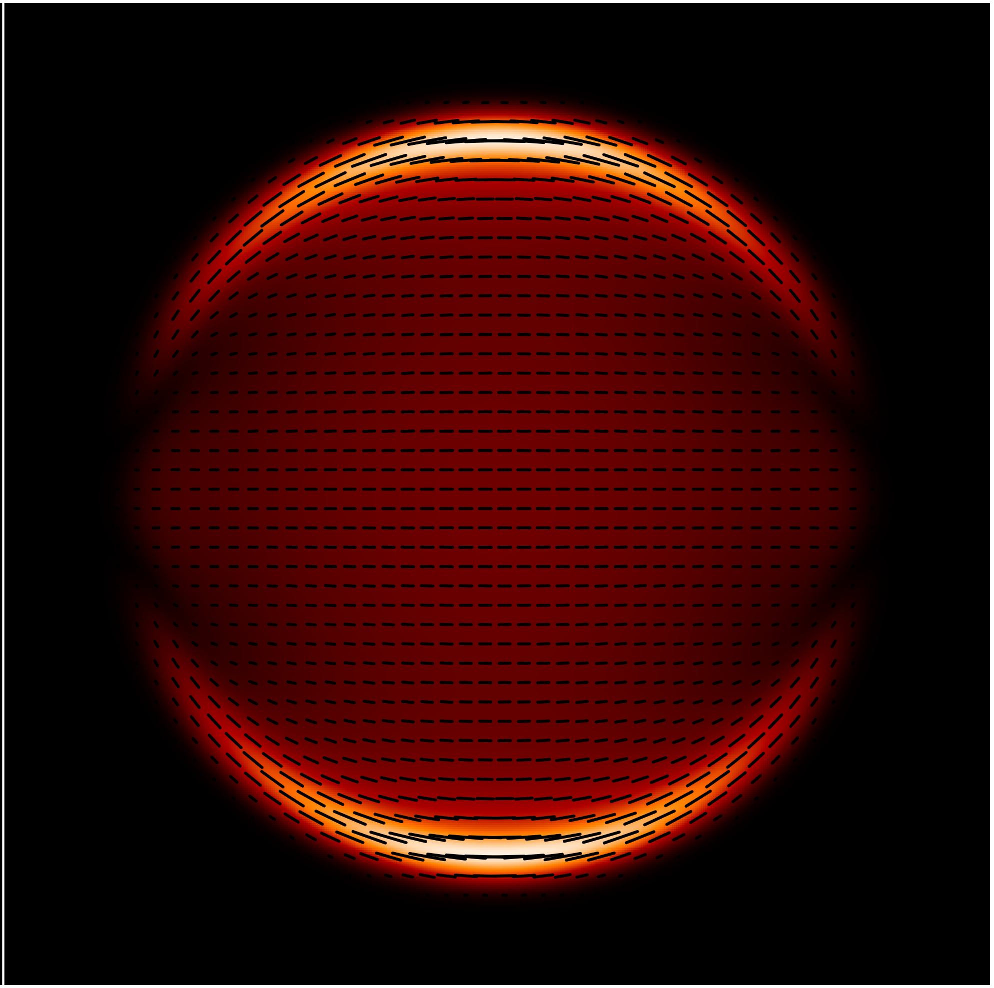

Emission Structure of SNRs

Rotation Angle $\Theta = 60^{\circ}$

Stokes I

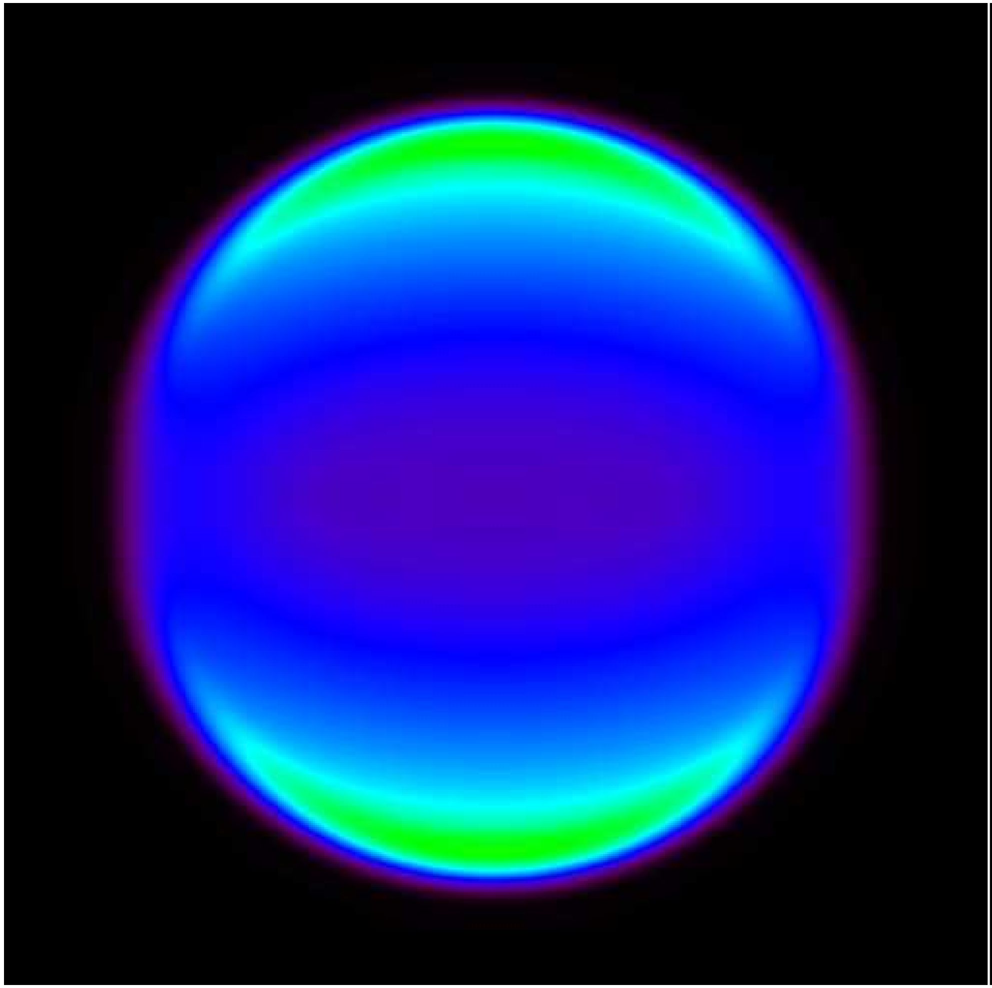

PI + B-vectors

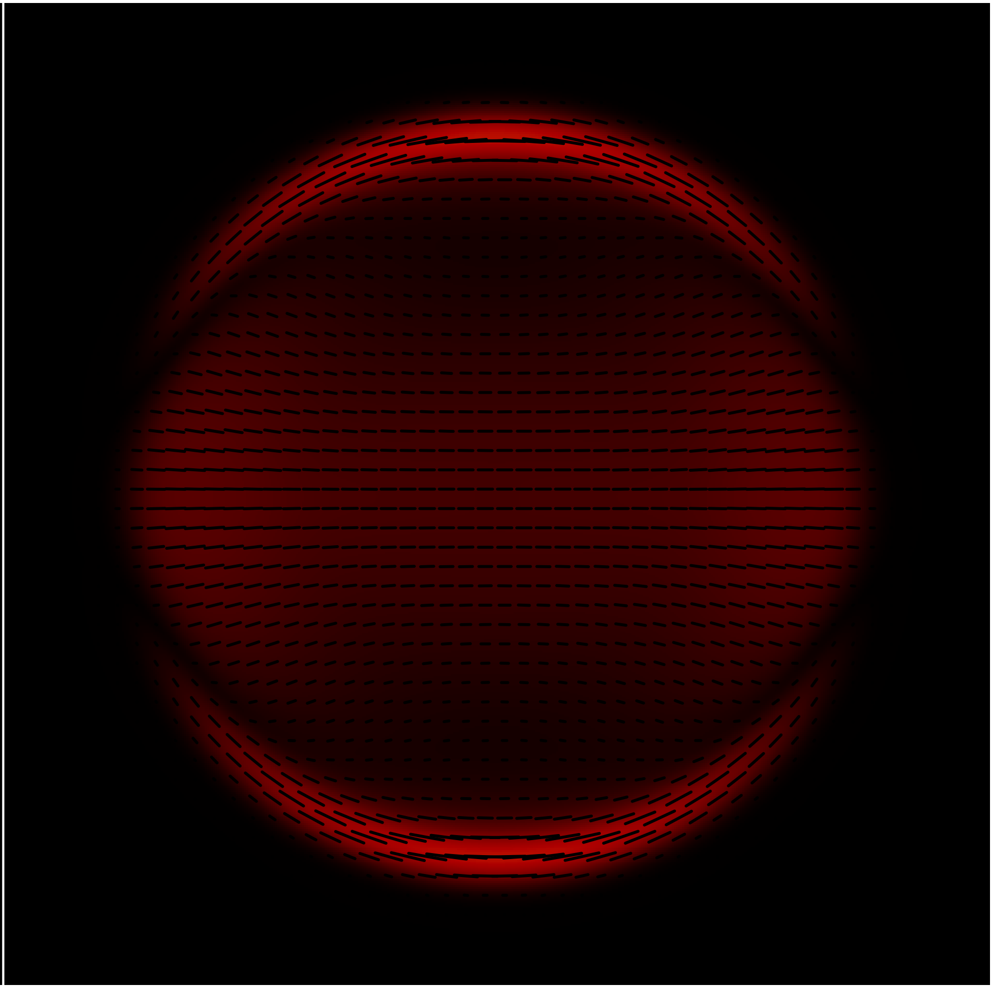

Emission Structure of SNRs

Rotation Angle $\Theta = 75^\circ$

Stokes I

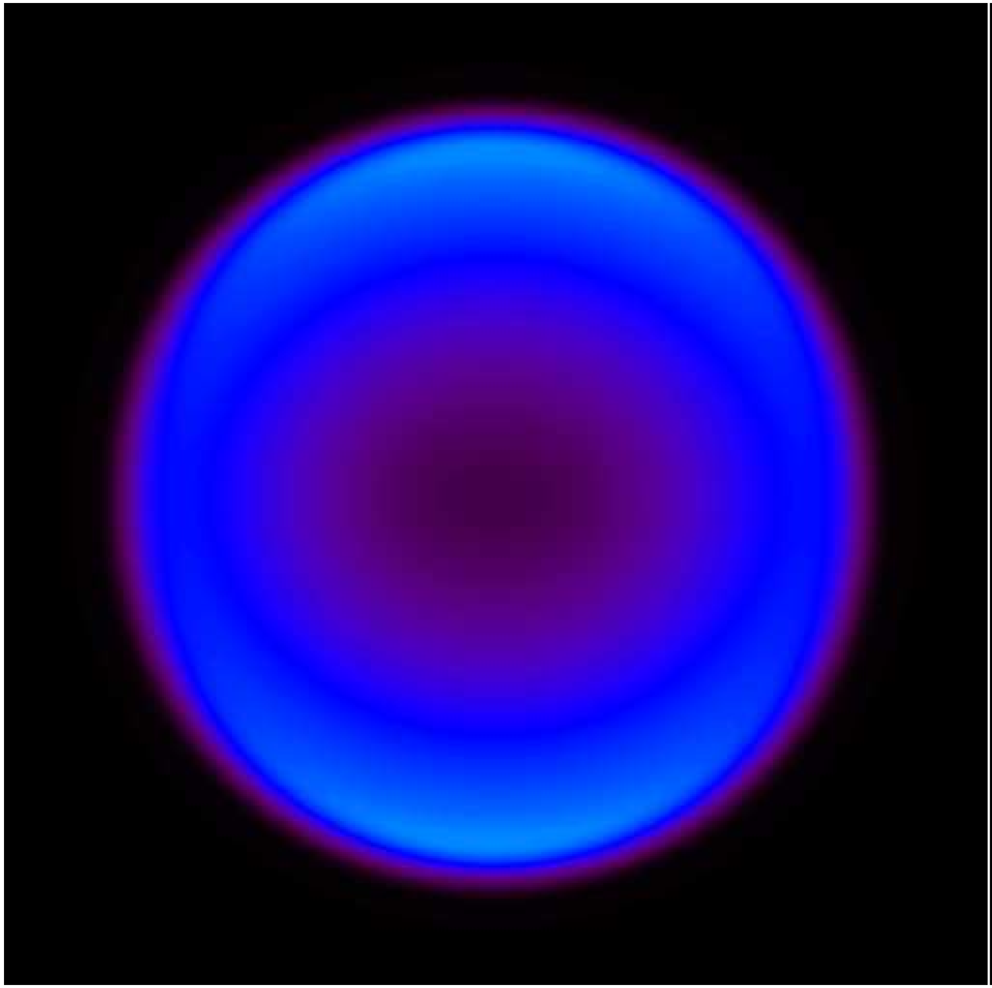

PI + B-vectors

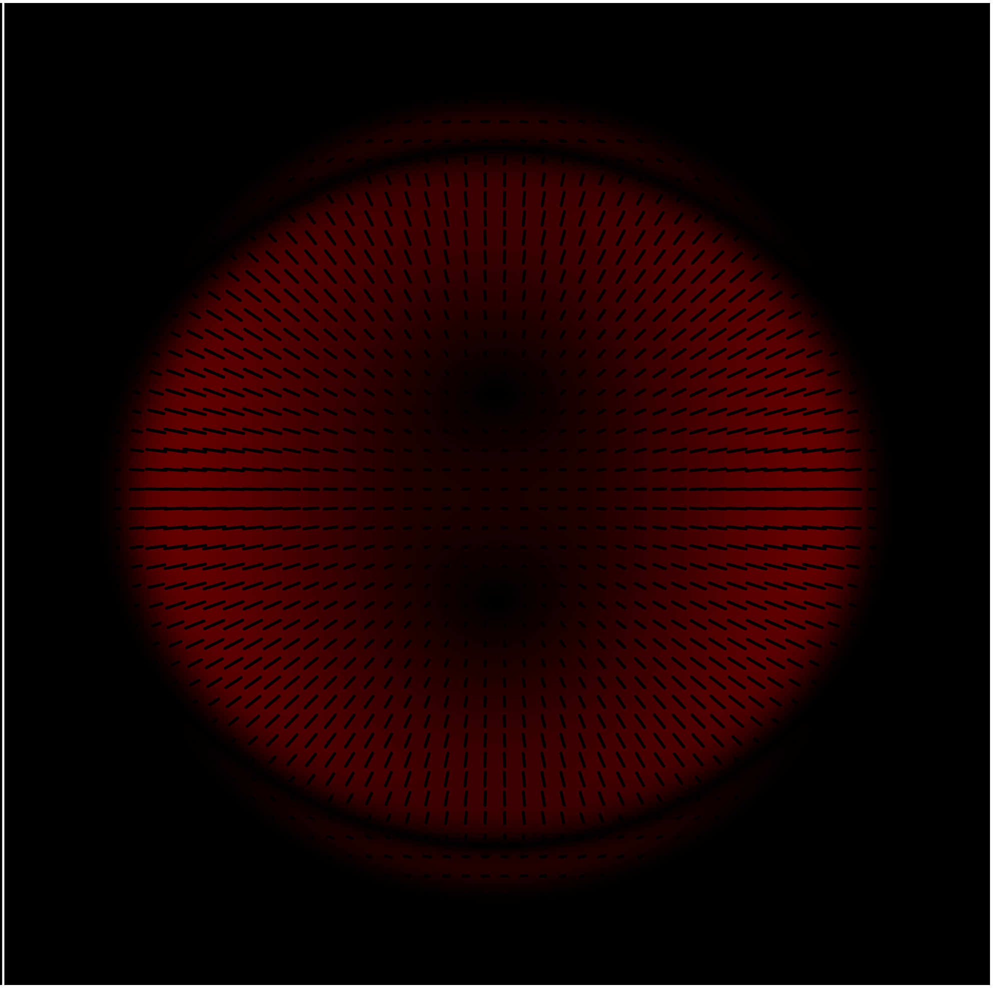

Emission Structure of SNRs

Rotation Angle $\Theta = 90^{\circ}$

Stokes I

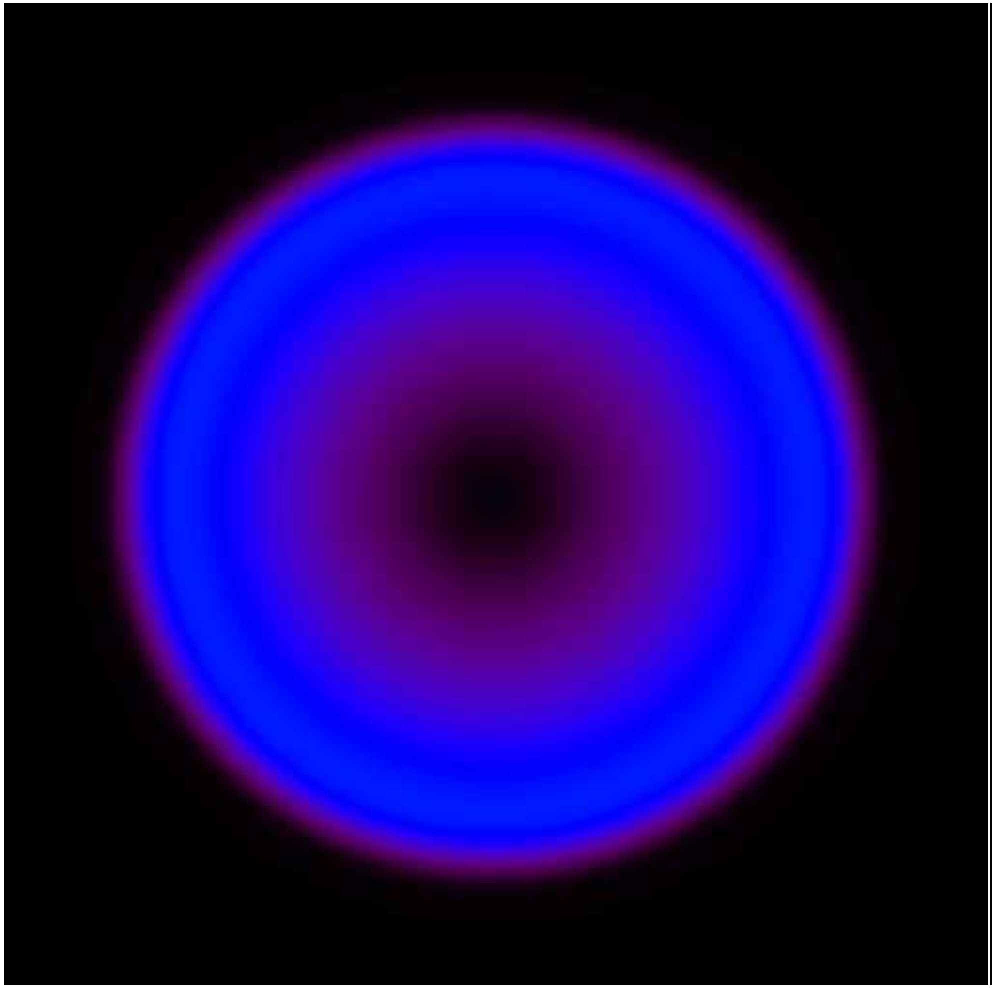

PI + B-vectors

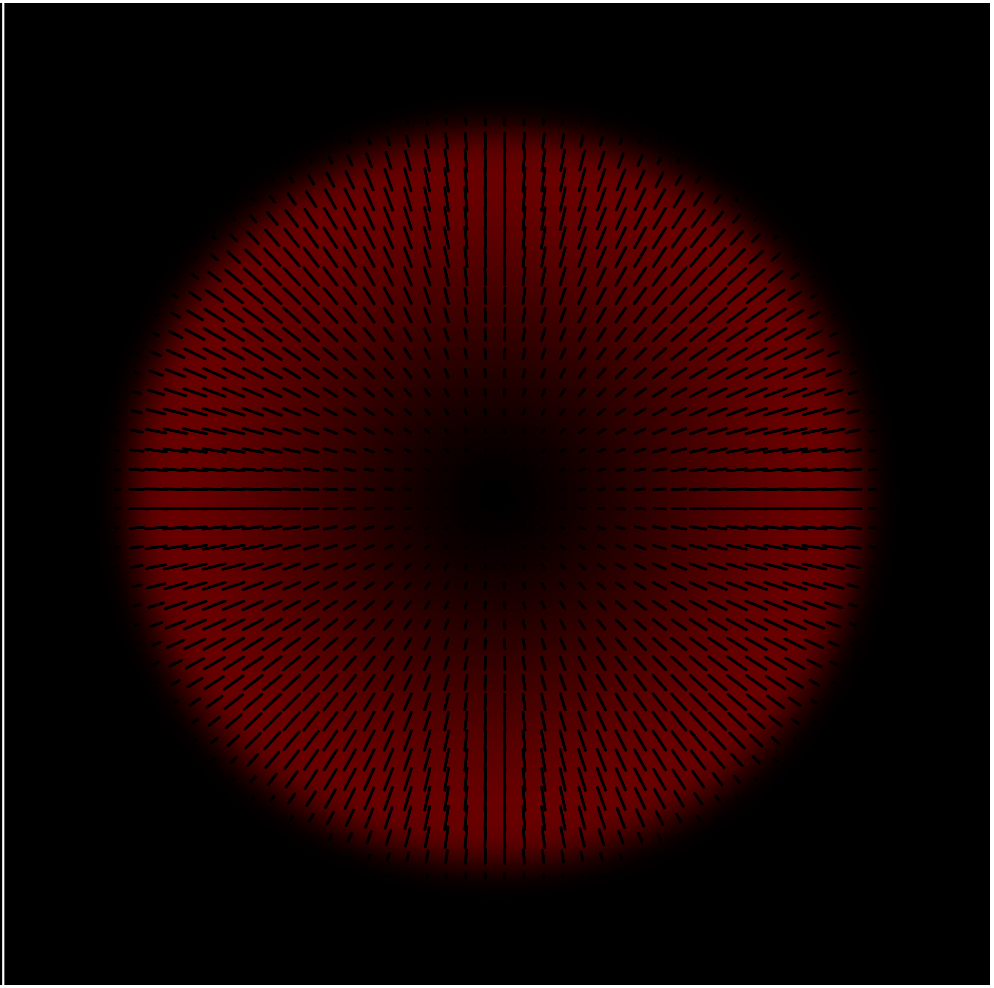

Emission Structure of SNRs

Rotation Angle $\Theta = 90^\circ$

Stokes I

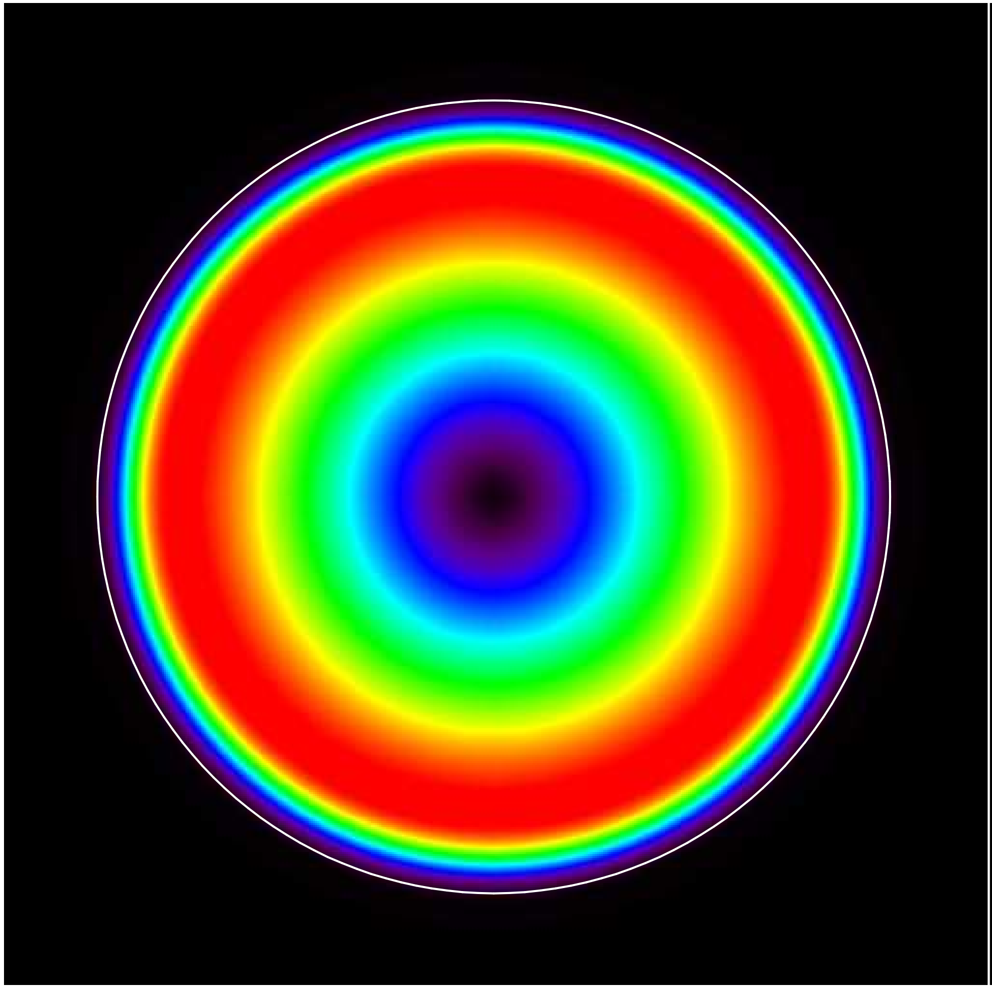

PI + B-vectors

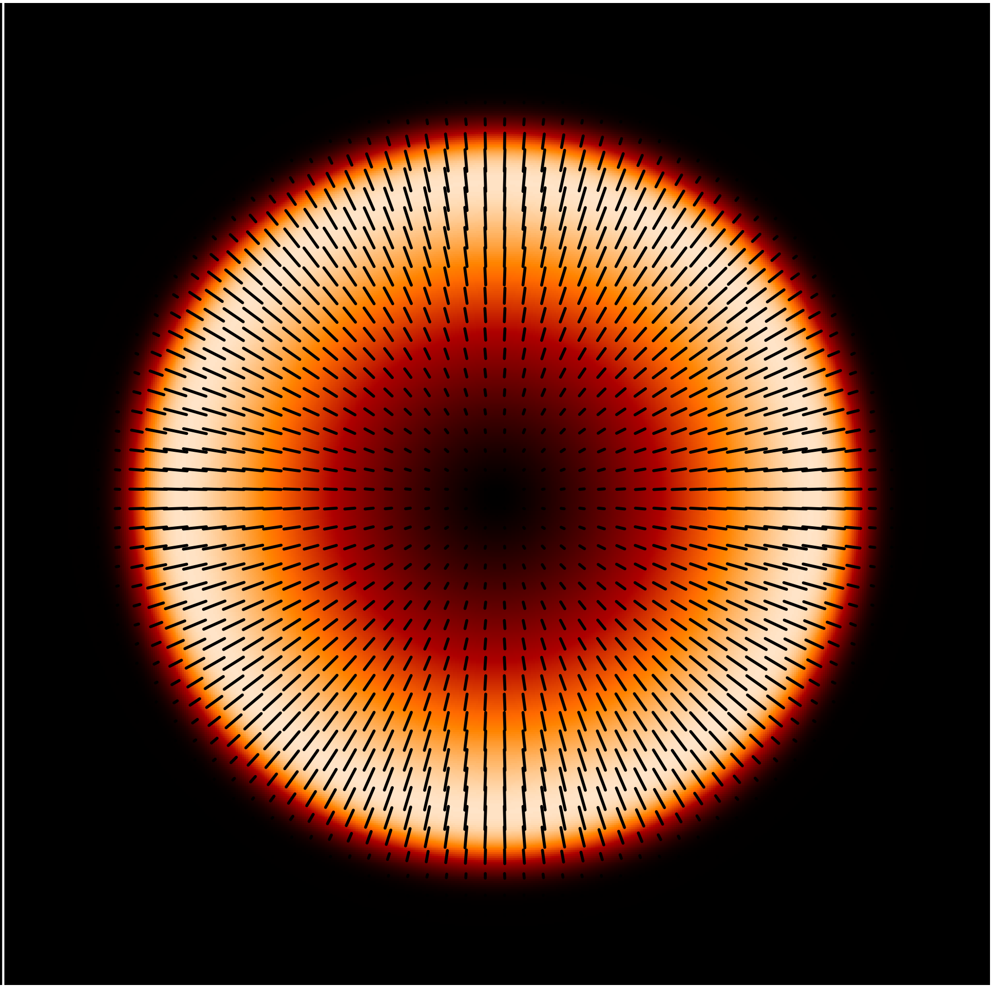

Rotation Angle $\Theta = 0^\circ$

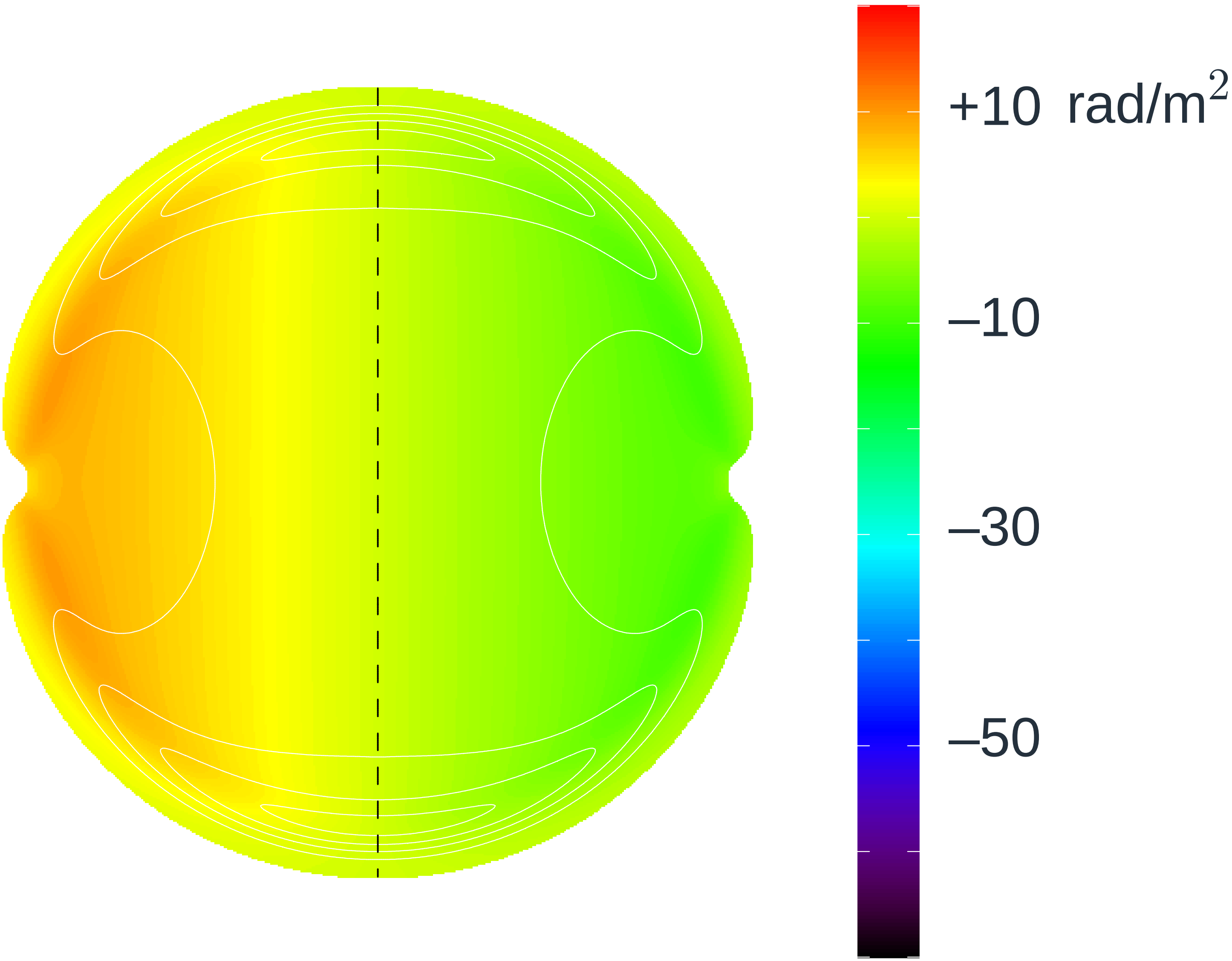

Faraday Rotation in SNRs

Rotation Angle $\Theta = 15^\circ$

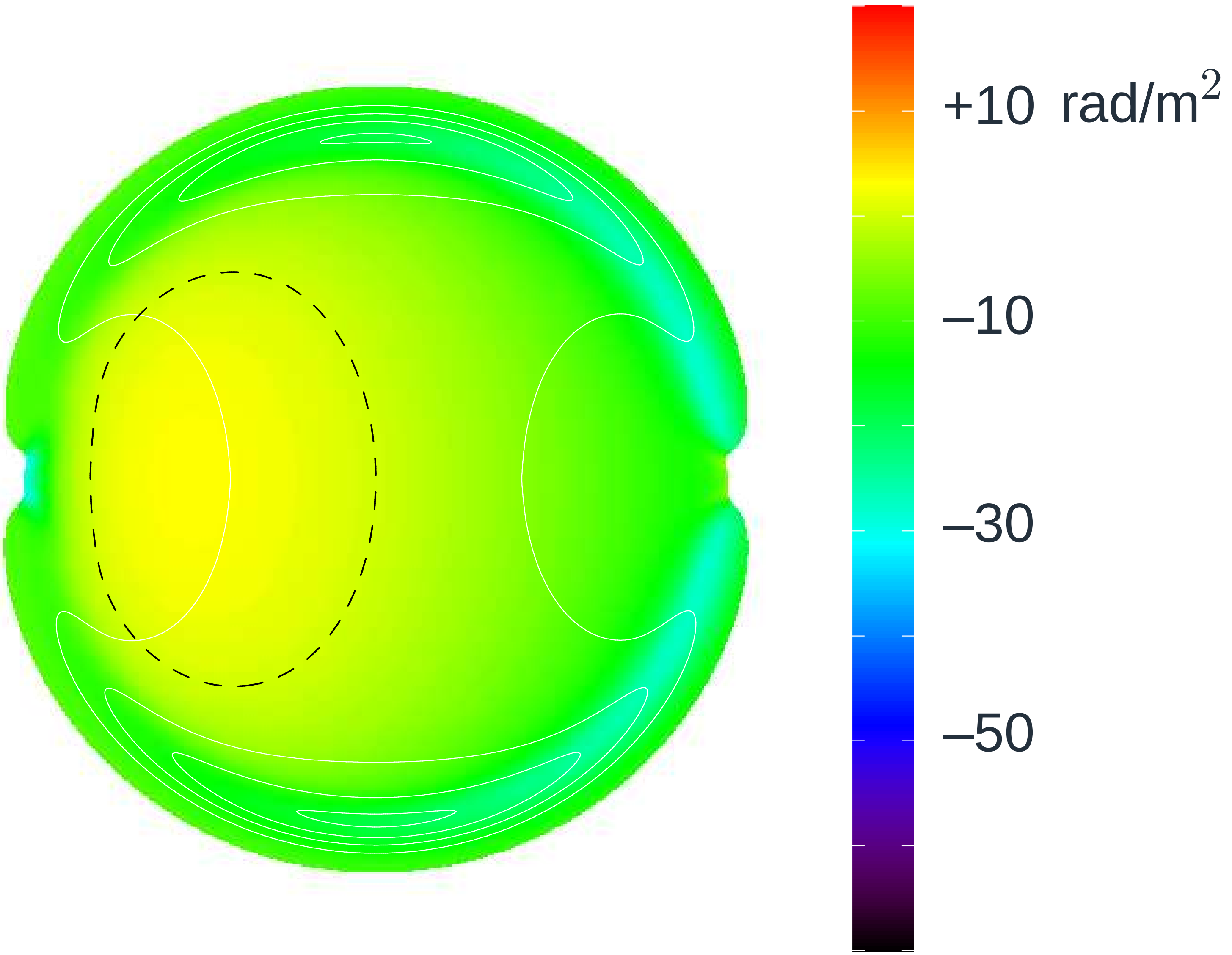

Faraday Rotation in SNRs

Rotation Angle $\Theta = 30^\circ$

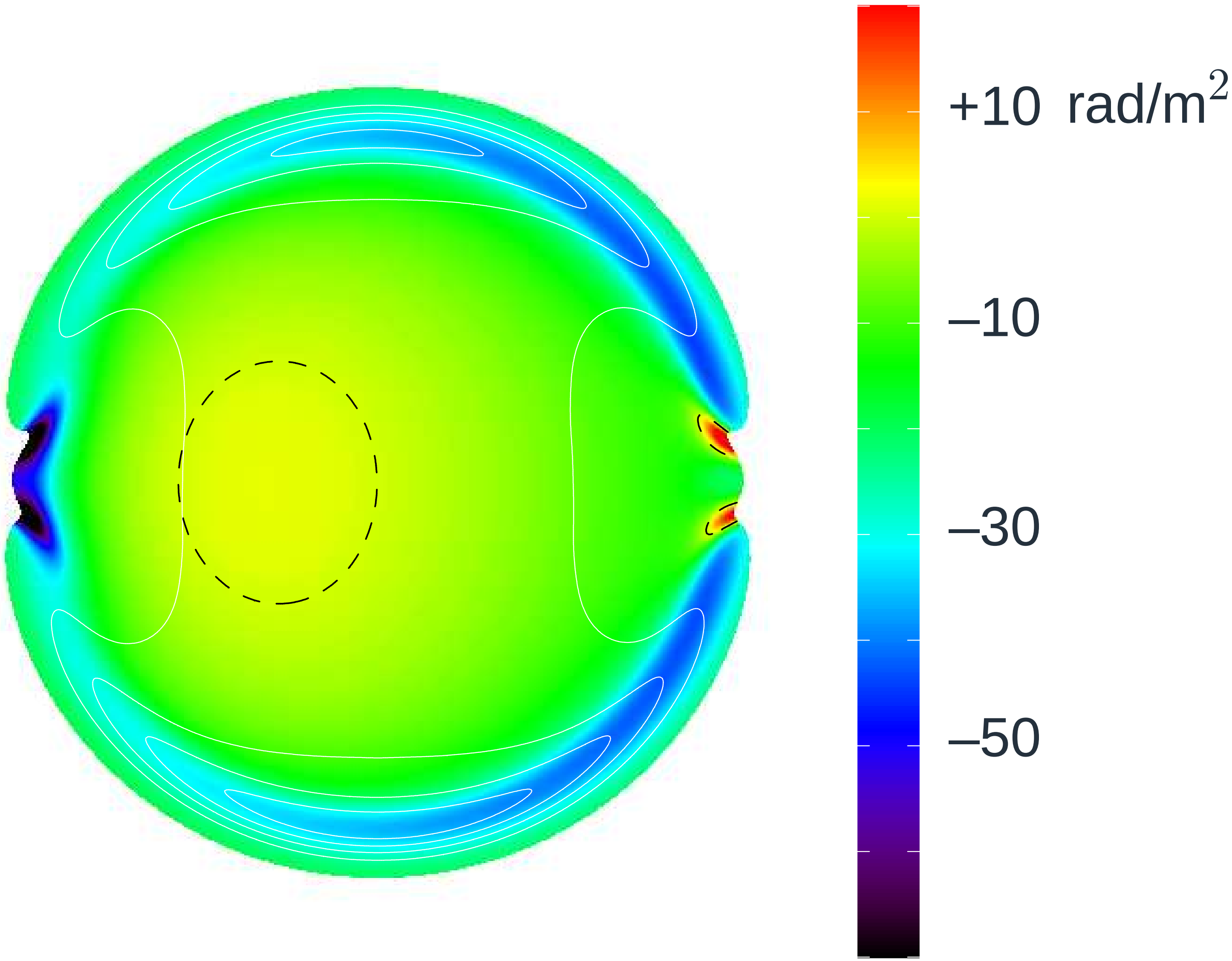

Faraday Rotation in SNRs

Rotation Angle $\Theta = 45^\circ$

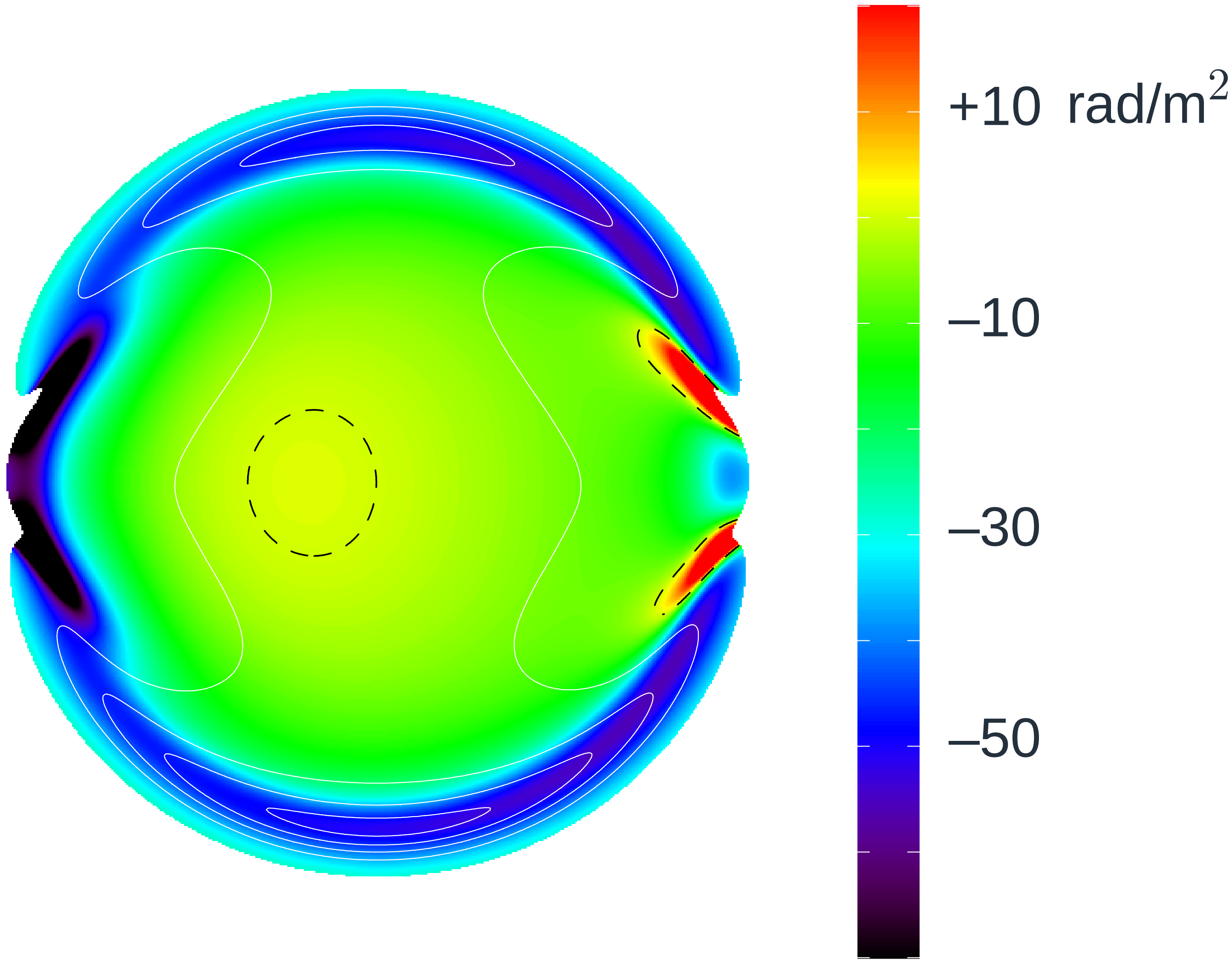

Rotation Angle $\Theta = 60^\circ$

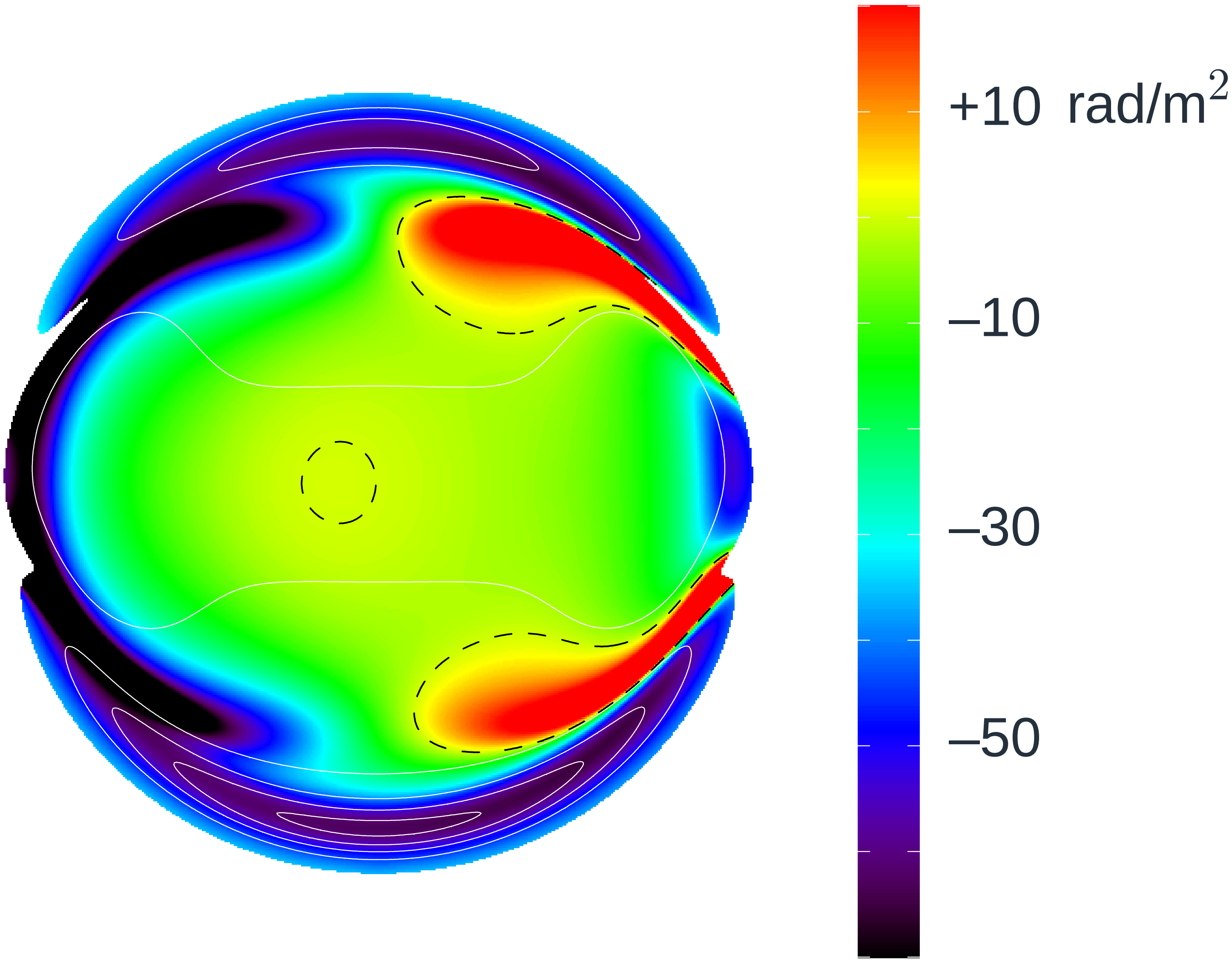

Rotation Angle $\Theta = 75°$

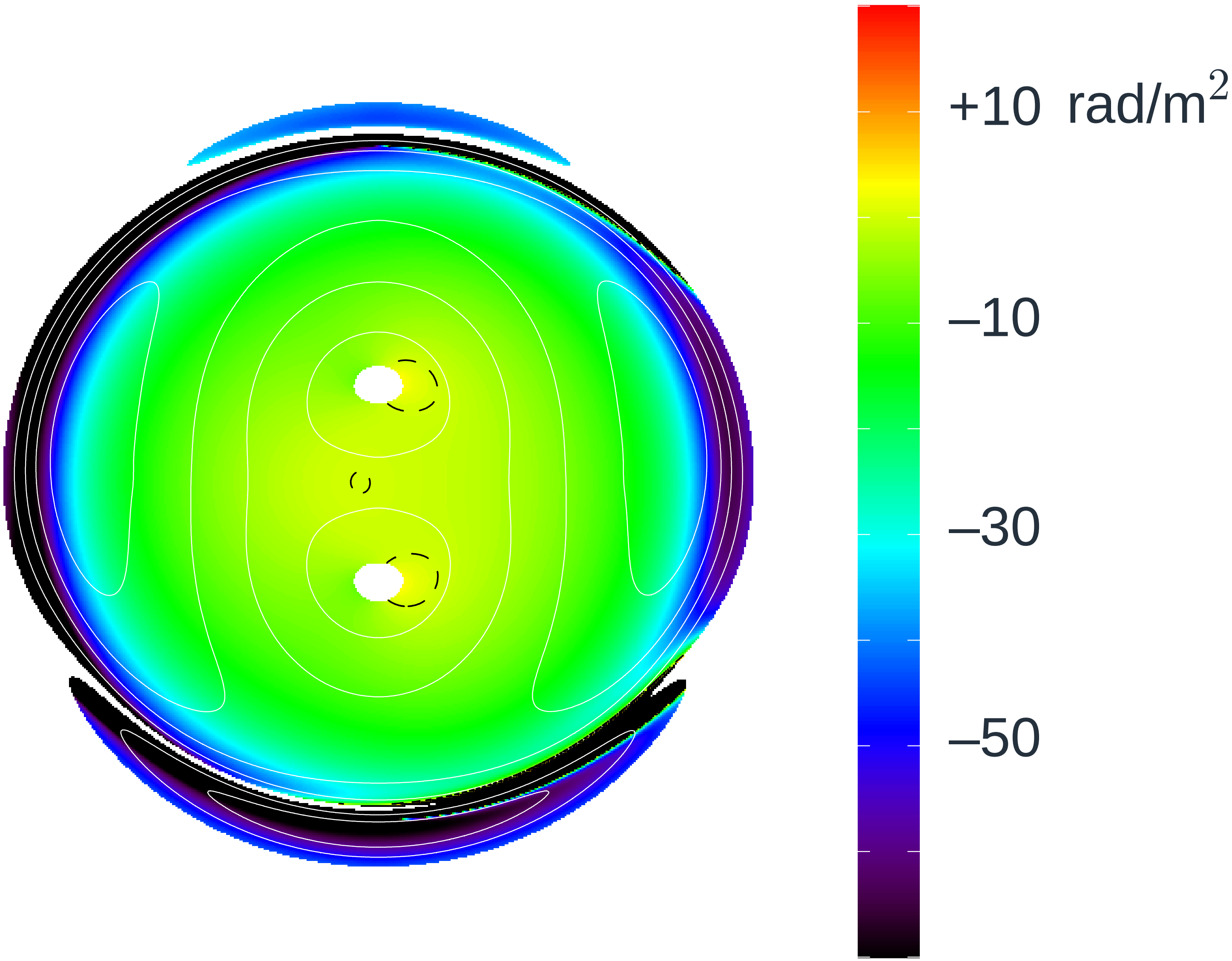

Rotation Angle $\Theta = 90^\circ$

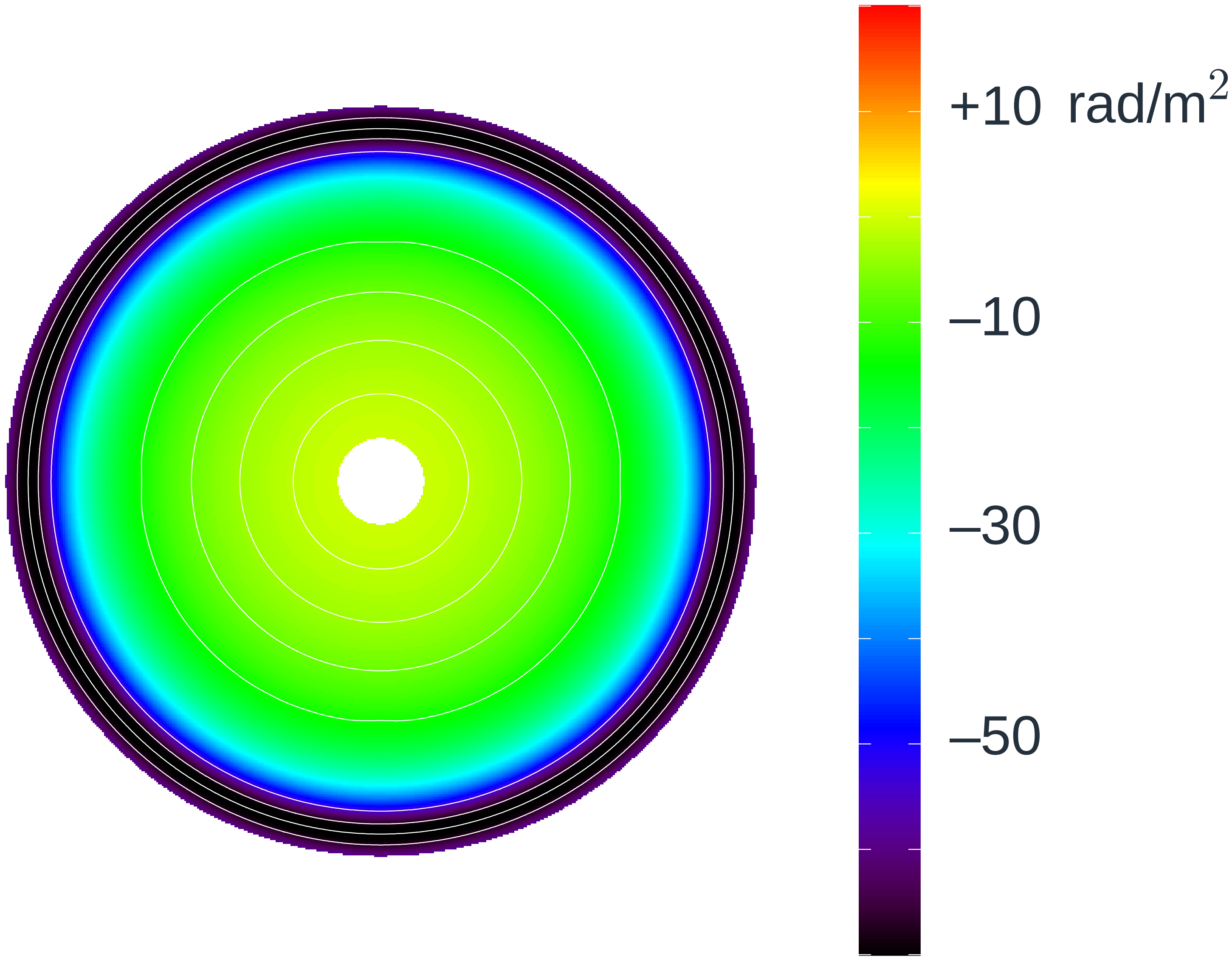

RM Gradient

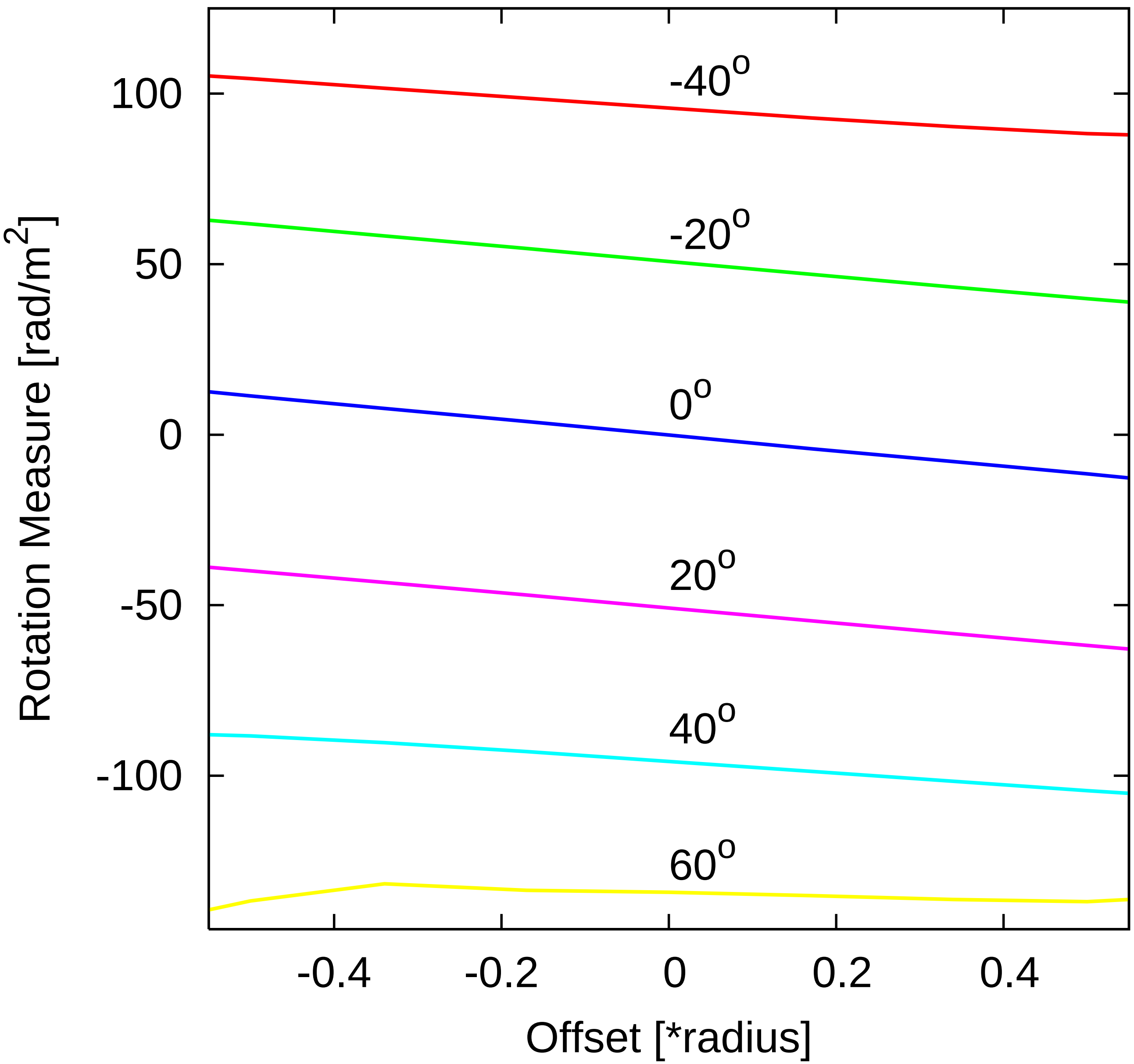
-40°
-20°
0°
20°
40°
60°
100
50
0
-50
-100
Rotation Measure [rad/m²]
-0.4
-0.2
0
0.2
0.4
Offset [*radius]

RM Gradient

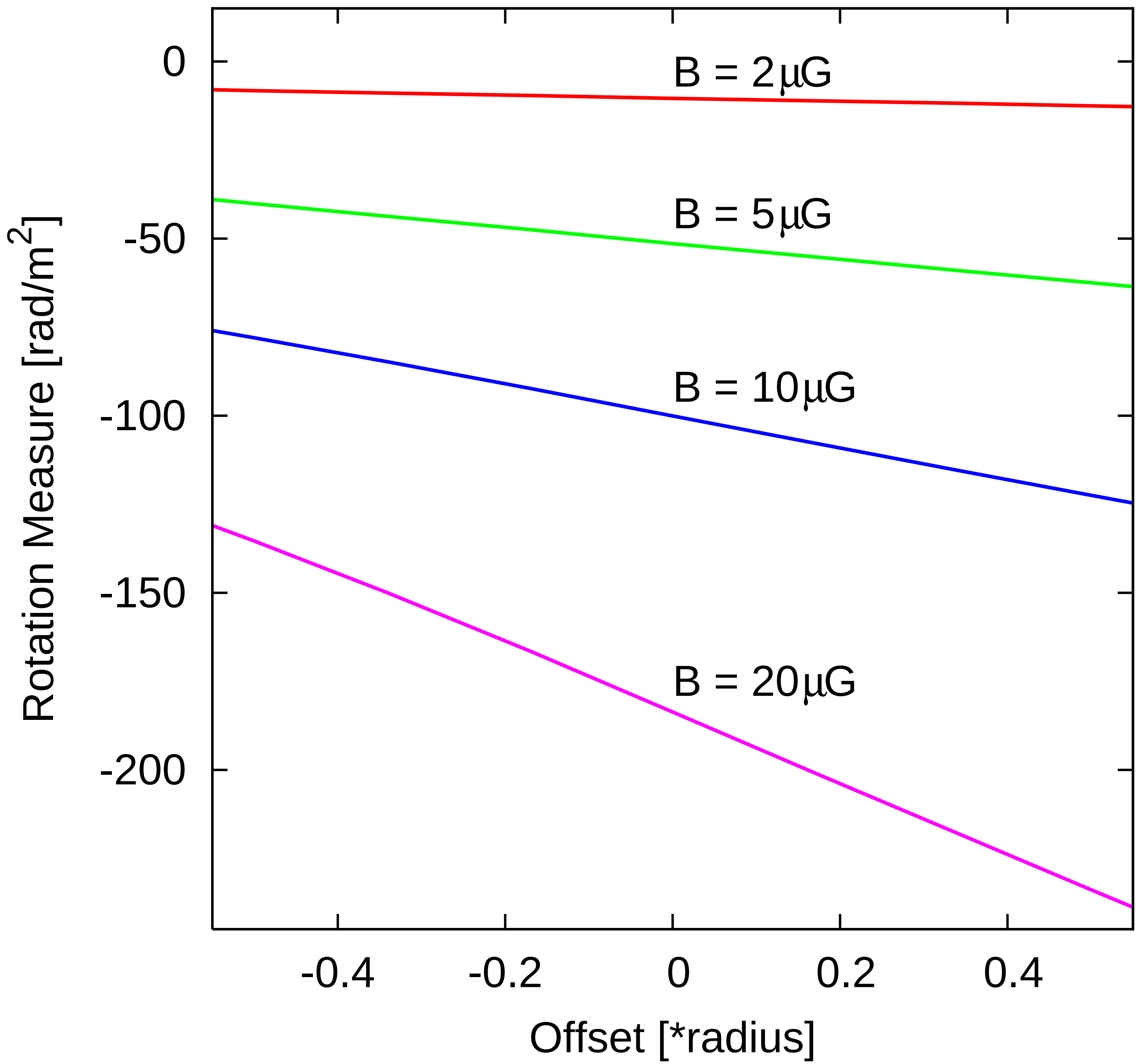
0
-50
-100
-150
-200
Rotation Measure [rad/m^2]
-0.4
-0.2
0
0.2
0.4
Offset [*radius]
B = 2μG
B = 5μG
B = 10μG
B = 20μG

DA 530 (G93.3+6.9)

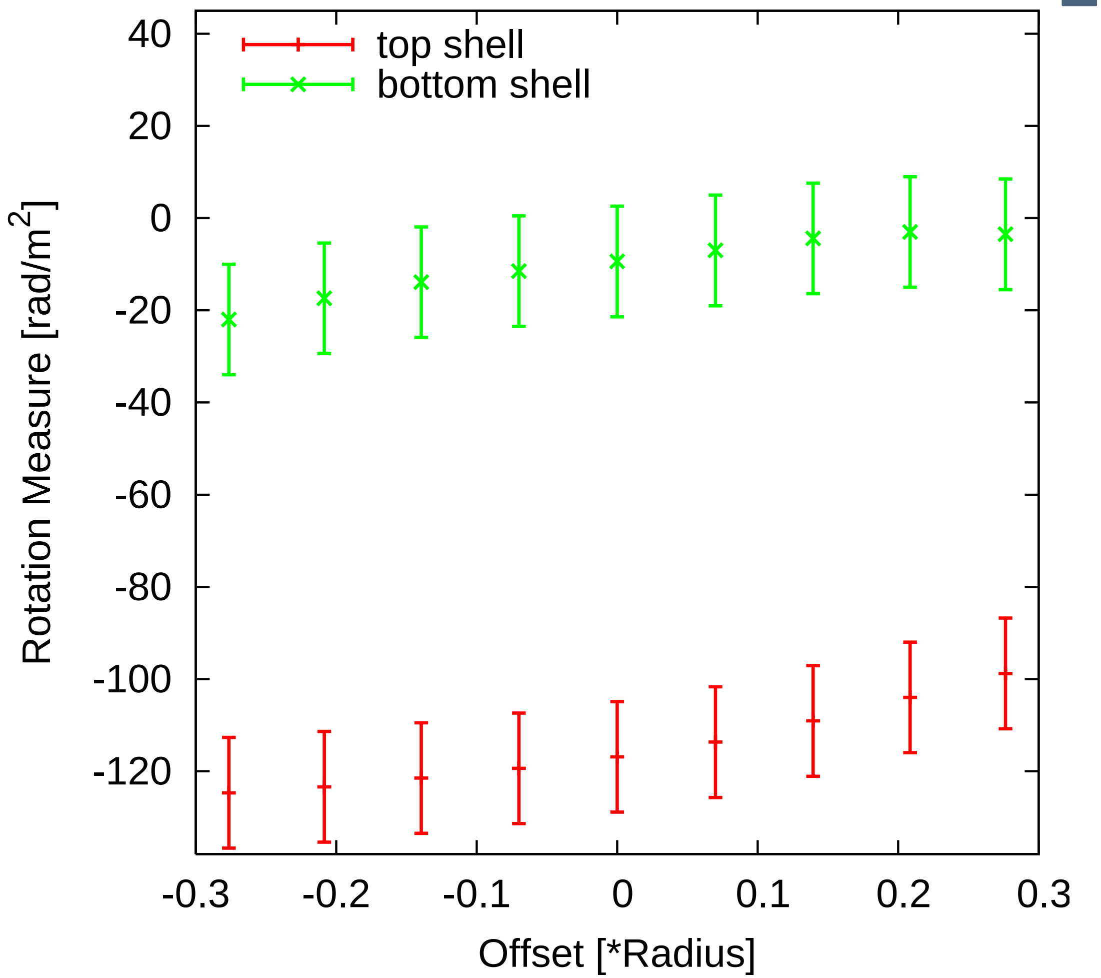

- The ambient B-field is pointing away from front left to back right.

DA 530 (G93.3+6.9)

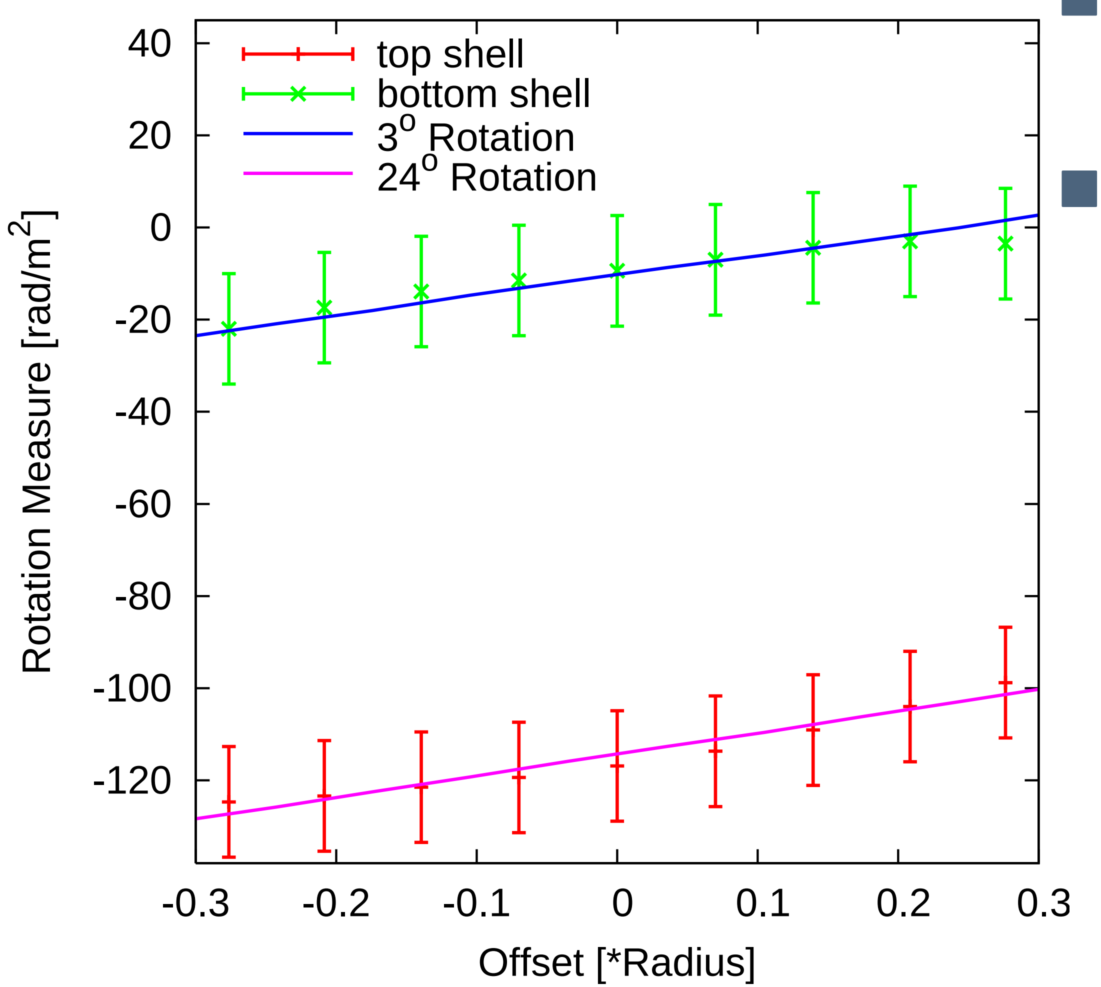

- The ambient B-field is pointing away from front left to back right.
- both shells show the same gradient $\Rightarrow$ same $B \cdot n_e$

DA 530 (G93.3+6.9)

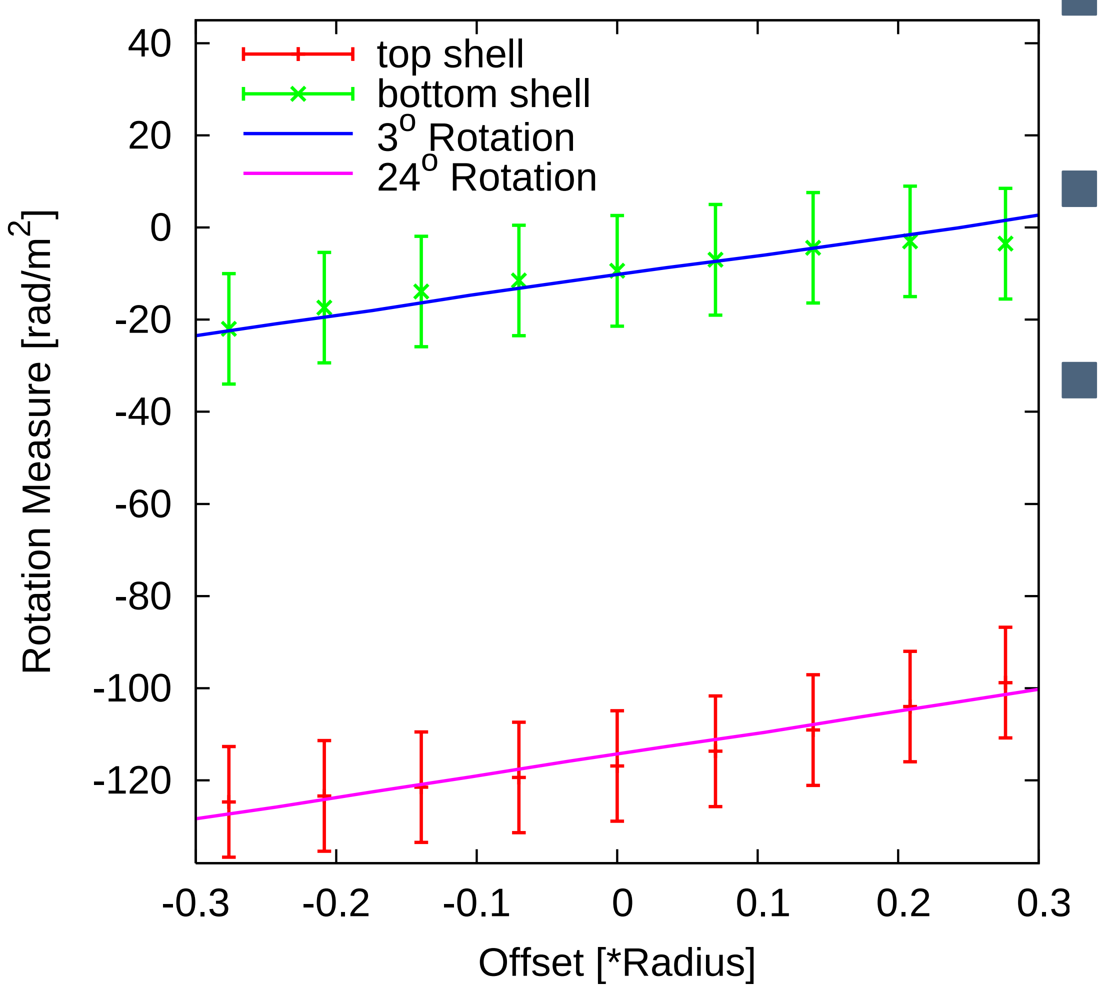

- The ambient B-field is pointing away from front left to back right.
- both shells show the same gradient $\Rightarrow$ same $B \cdot n_e$
- The top shell expands in a B-field with $\Theta = 24°$, the bottom shell with $\Theta = 3°$.

  $\Rightarrow$ The ambient B-field is twisted counter-clockwise.

DA 530 (G93.3+6.9)

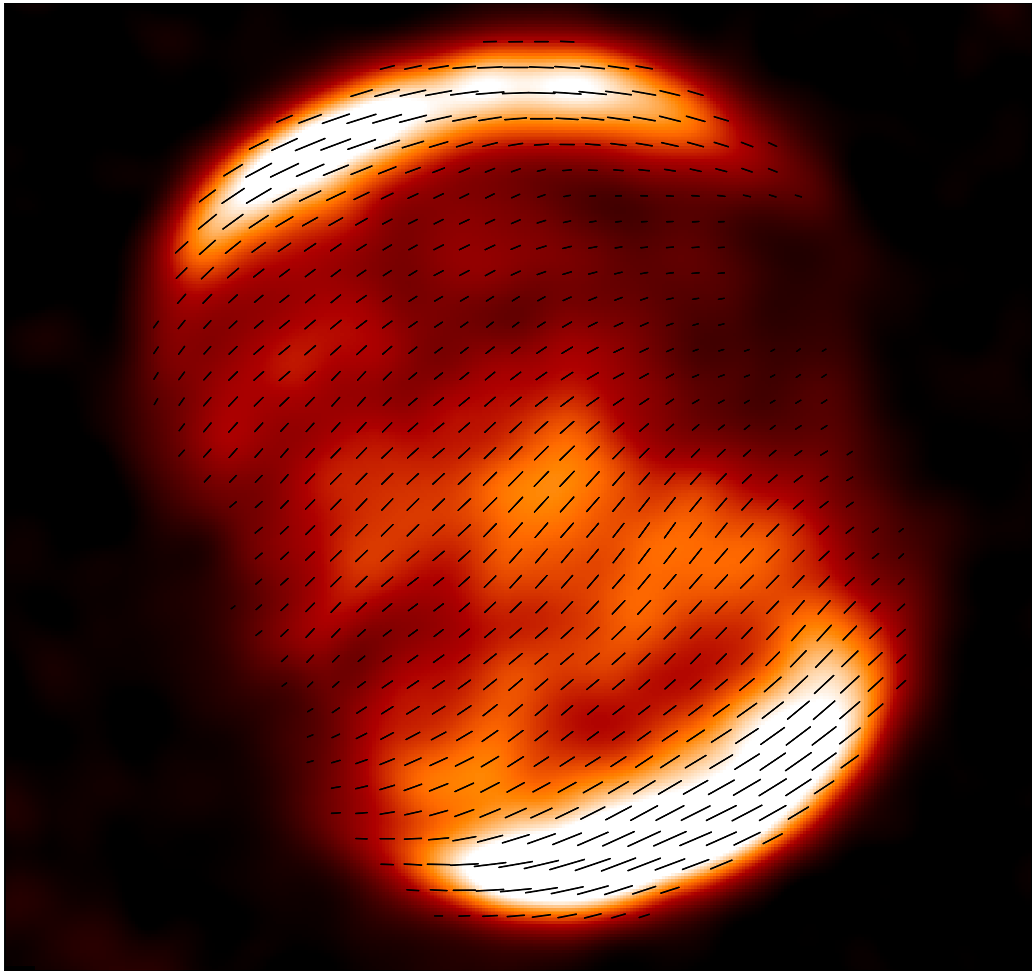

- The ambient B-field is pointing away from front left to back right.
- both shells show the same gradient $\Rightarrow$ same $B \cdot n_e$
- The top shell expands in a B-field with $\Theta = 24°$, the bottom shell with $\Theta = 3°$.

  $\Rightarrow$ The ambient B-field is twisted counter-clockwise.
- The lower surface brightness of the top shell confirms this.

DA 530 (G93.3+6.9)

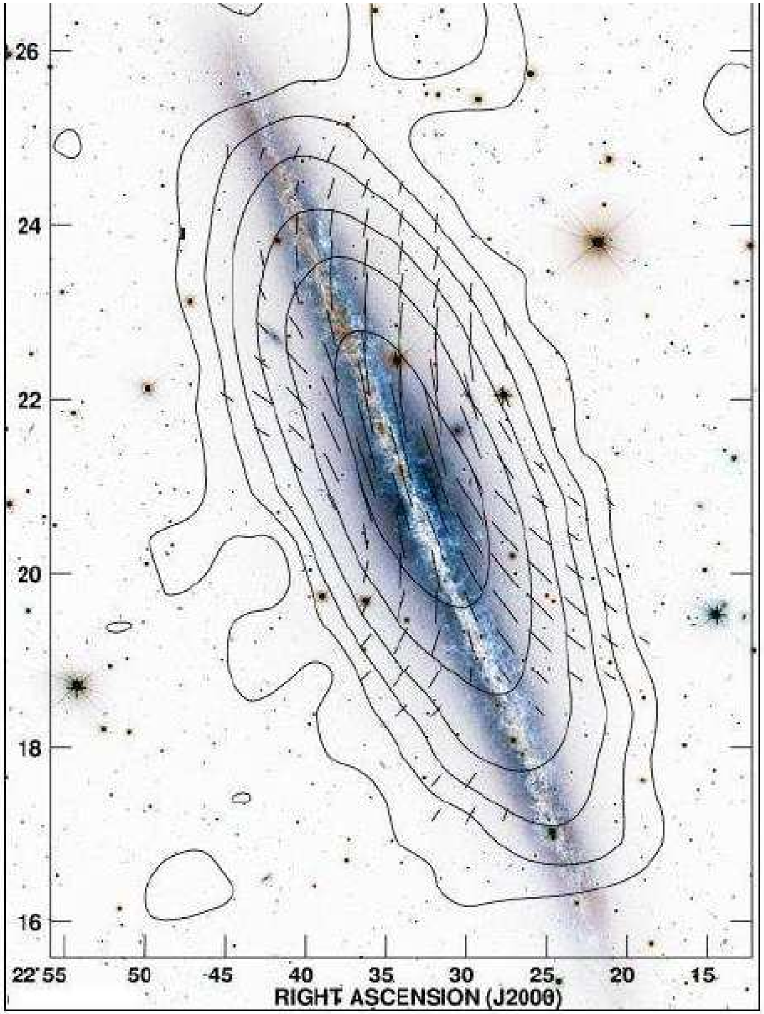

- Radio observations of other galaxies show twisted magnetic spurs emerging from star forming regions (e.g.: Review by Beck, 2008: Galactic dynamos and galactic winds).

DA 530 (G93.3+6.9)

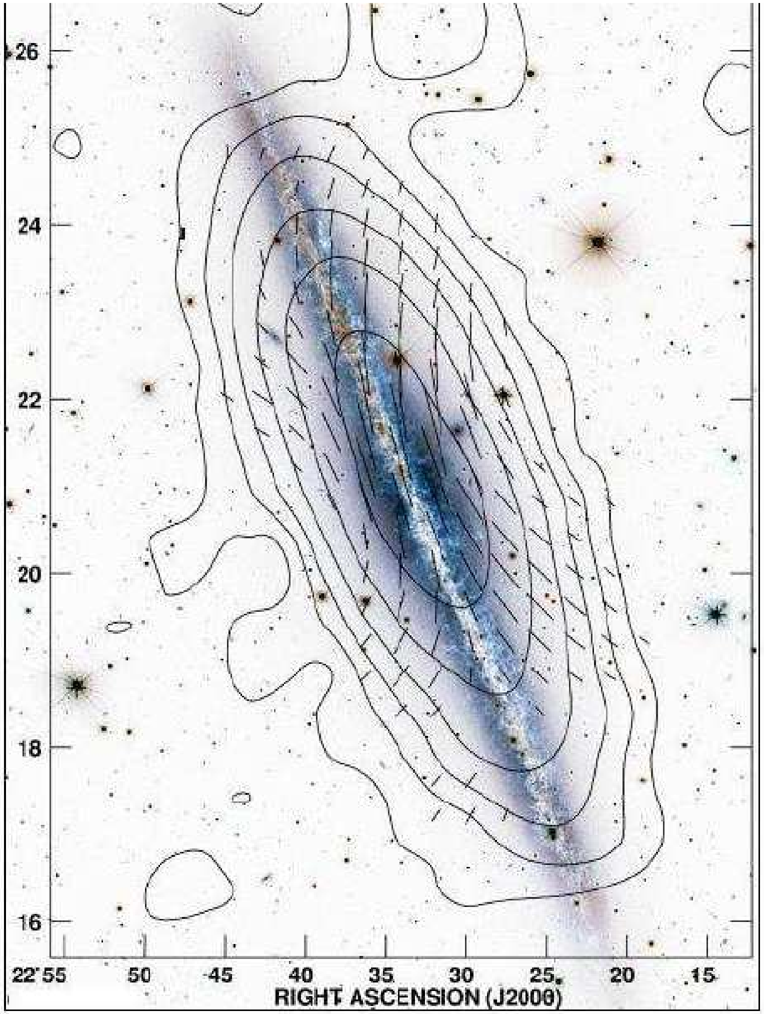

- Radio observations of other galaxies show twisted magnetic spurs emerging from star forming regions (e.g.: Review by Beck, 2008: Galactic dynamos and galactic winds).
- DA 530 is located above an area of the Milky Way, which is rich in star forming regions, HII regions, and supernova remnants.

DA 530 (G93.3+6.9)

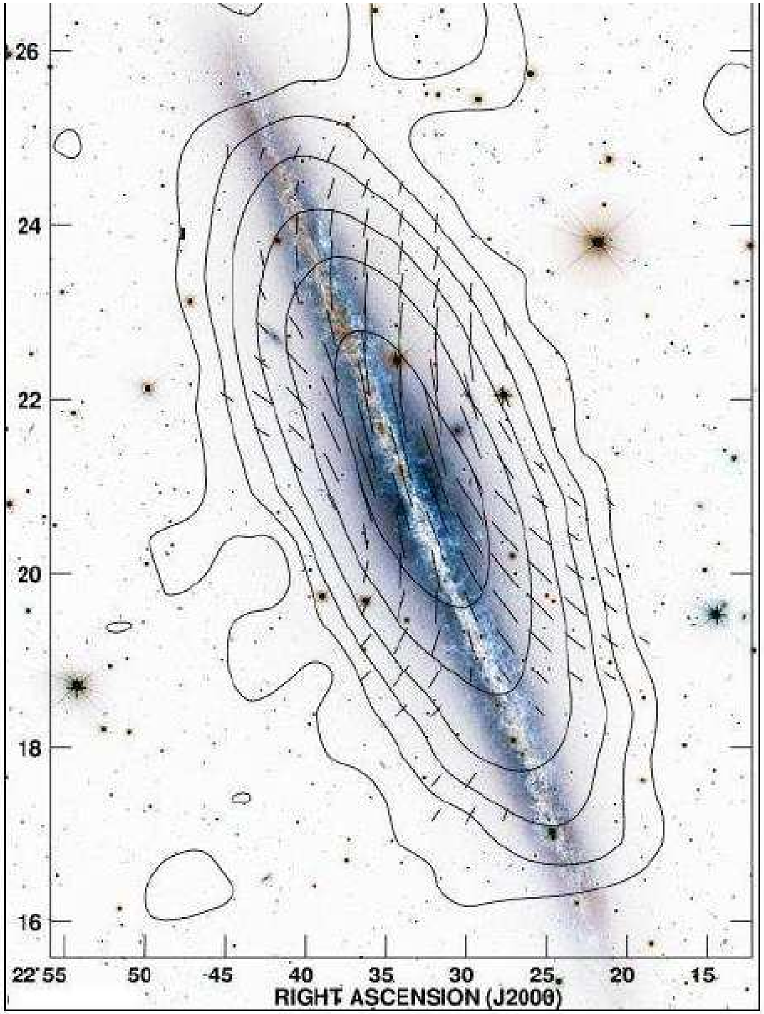

- Radio observations of other galaxies show twisted magnetic spurs emerging from star forming regions (e.g.: Review by Beck, 2008: Galactic dynamos and galactic winds).
- DA 530 is located above an area of the Milky Way, which is rich in star forming regions, HII regions, and supernova remnants.
- Is DA 530 expanding inside these twisted magnetic spurs?

DA 530 in the Milky Way Galaxy

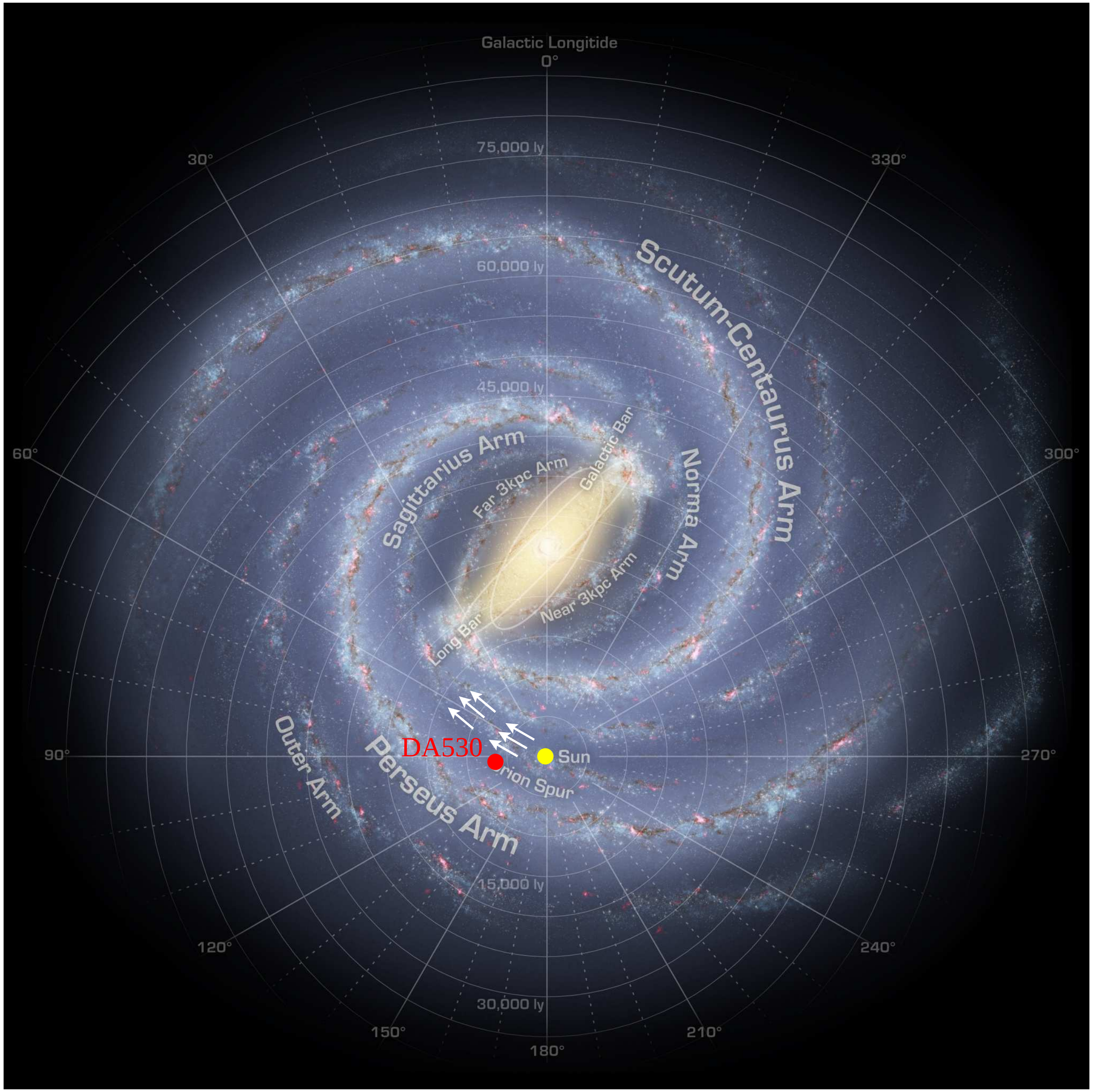

DA 495

Combined CGPS + NVSS image at 1420 MHz:

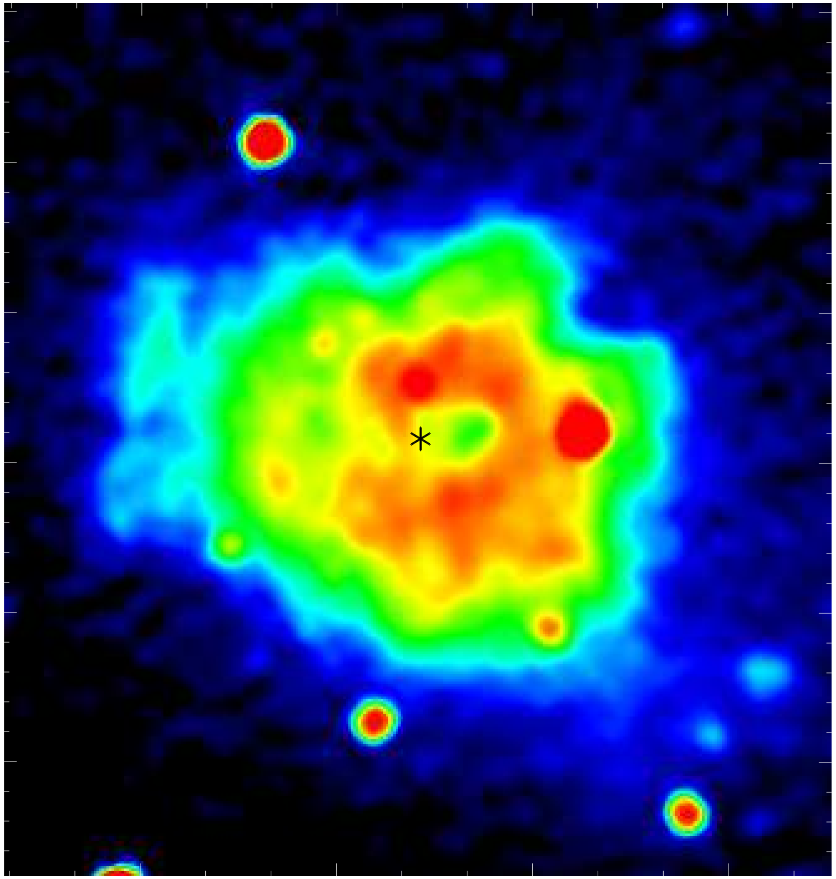

- DA 495 is a pulsar wind nebula with a recently discovered neutron star in the center.

Arzoumanian, Safi-Harb, Landecker, & Kothes, 2004, ApJ 610, L101

Combined CGPS + NVSS image at 1420 MHz:

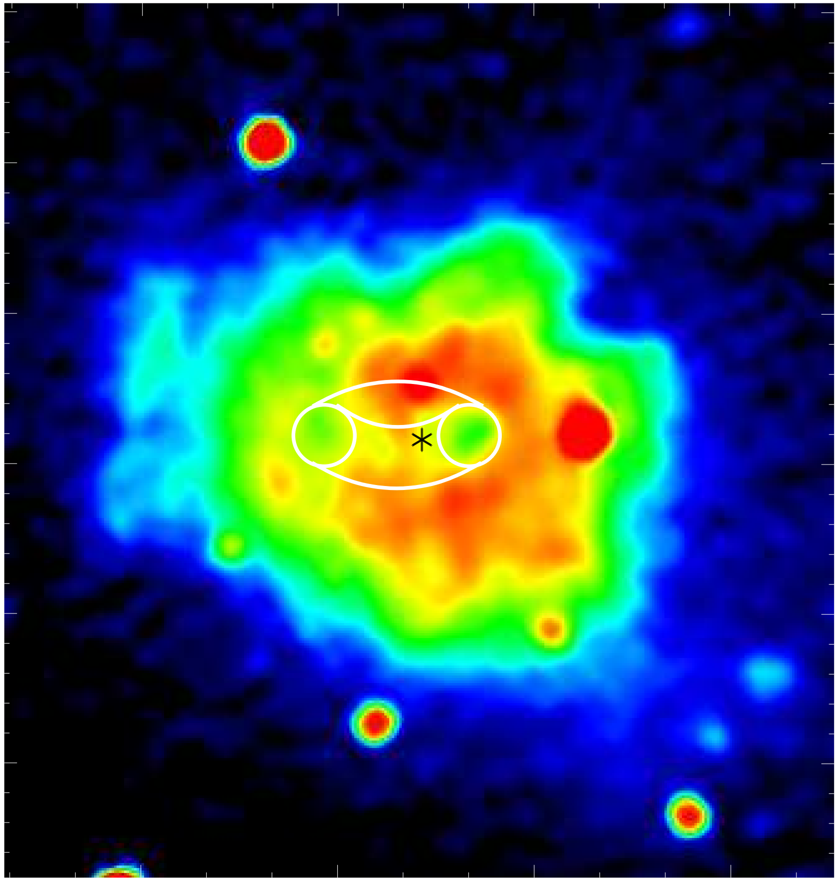

- DA 495 is a pulsar wind nebula with a recently discovered neutron star in the center.
- We believe the two holes indicate an equatorial torus of material ejected by the progenitor star.

Kothes, Landecker, Reich, Safi-Harb, & Arzoumanian, 2008, ApJ 687, 516

A Model of a Mature SNR

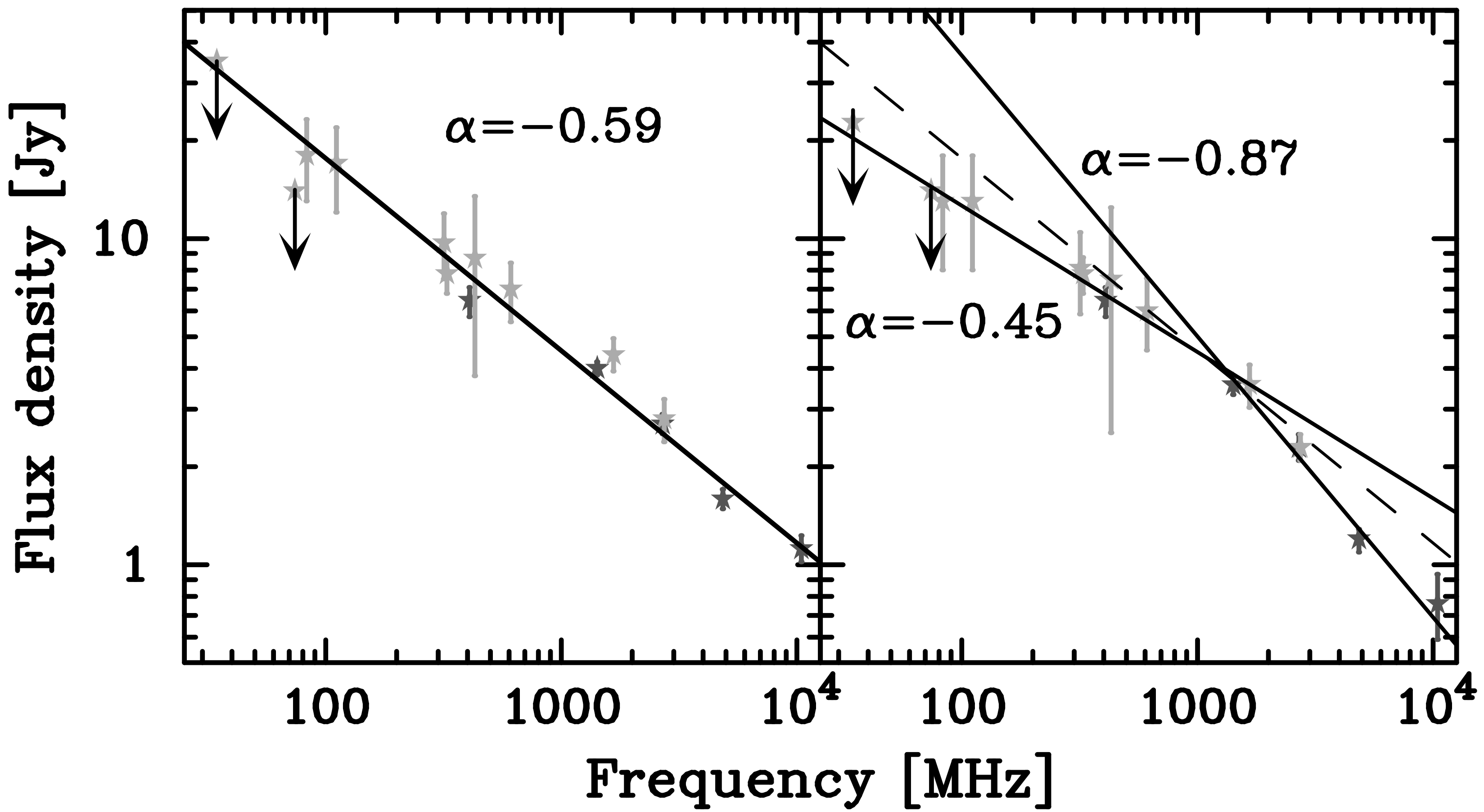

Age ≈ 20000 years, Magnetic field ≈ 1.3 mG

DA 495

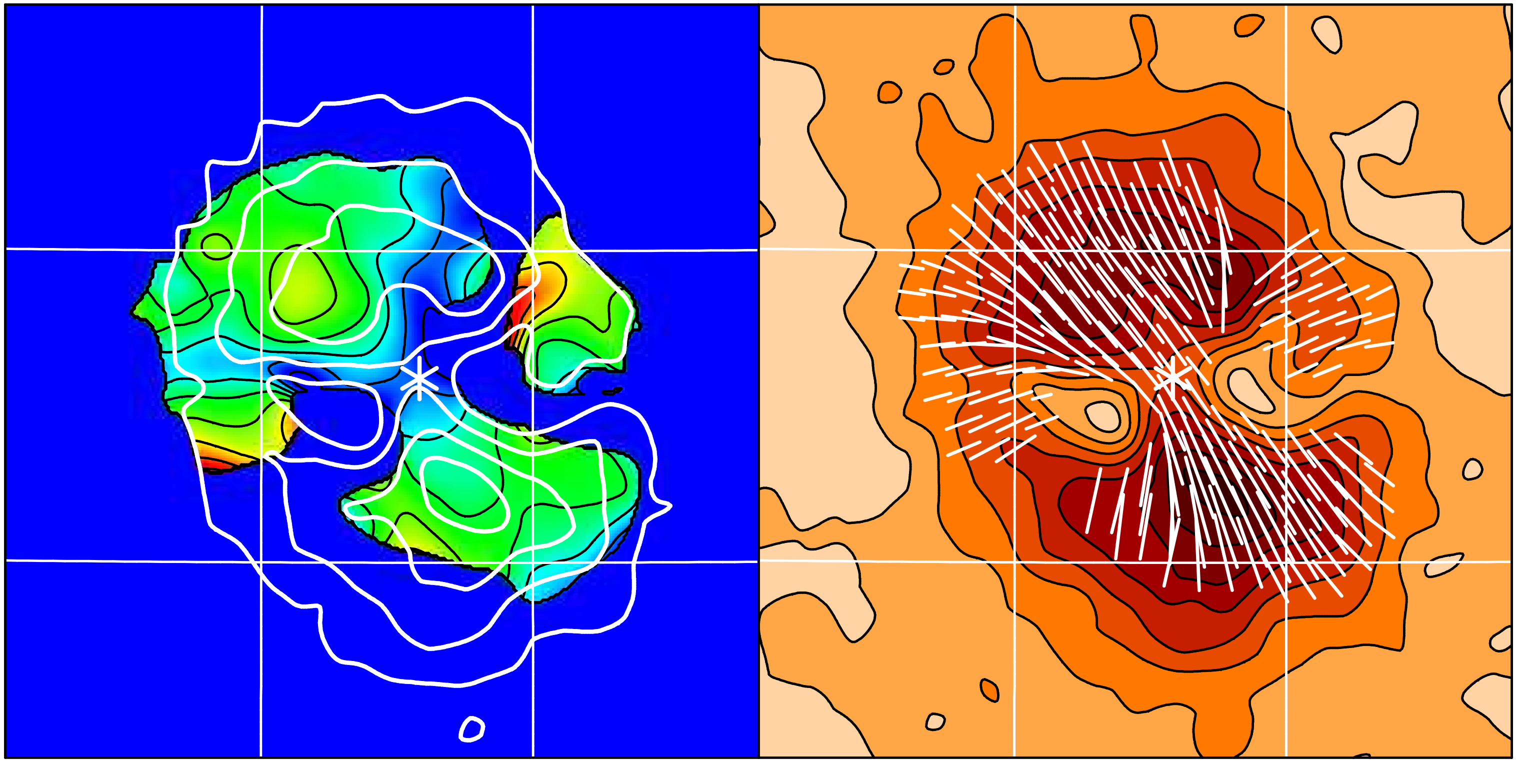

The first impression of the polarized emission is that of a remarkable bipolar structure centered at the pulsar. The B-vectors corrected for Faraday rotation indicate a dipole field inside the nebula.

Kothes, Landecker, Reich, Safi-Harb, & Arzoumanian, 2008, ApJ 687, 516

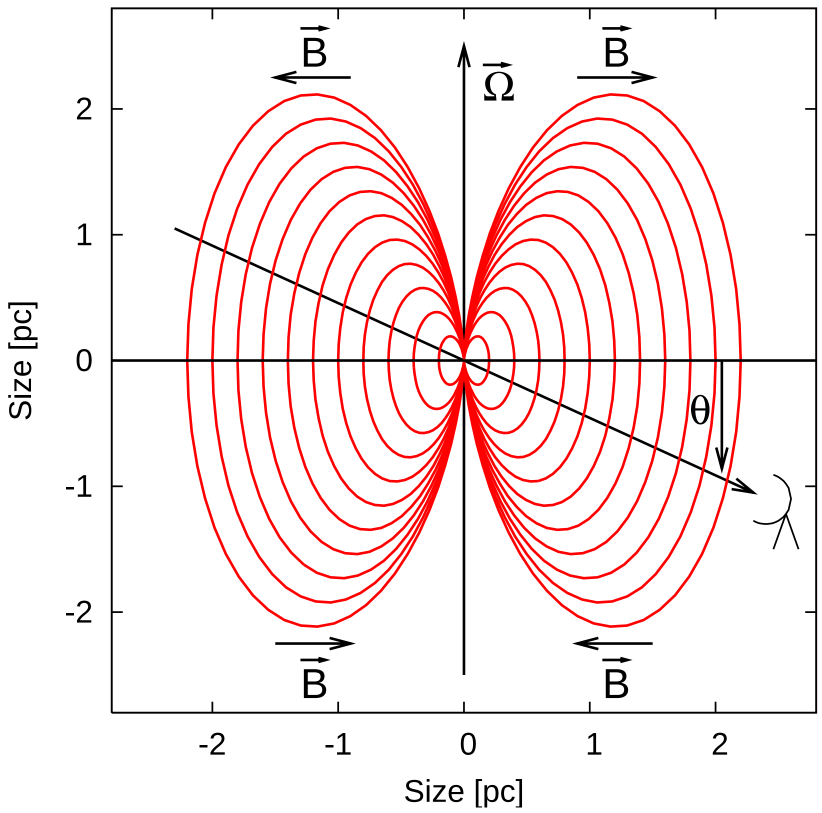

- Assuming that a dipole field is responsible for the Faraday rotation inside DA 495 we fitted this model to the RM map.

DA 495

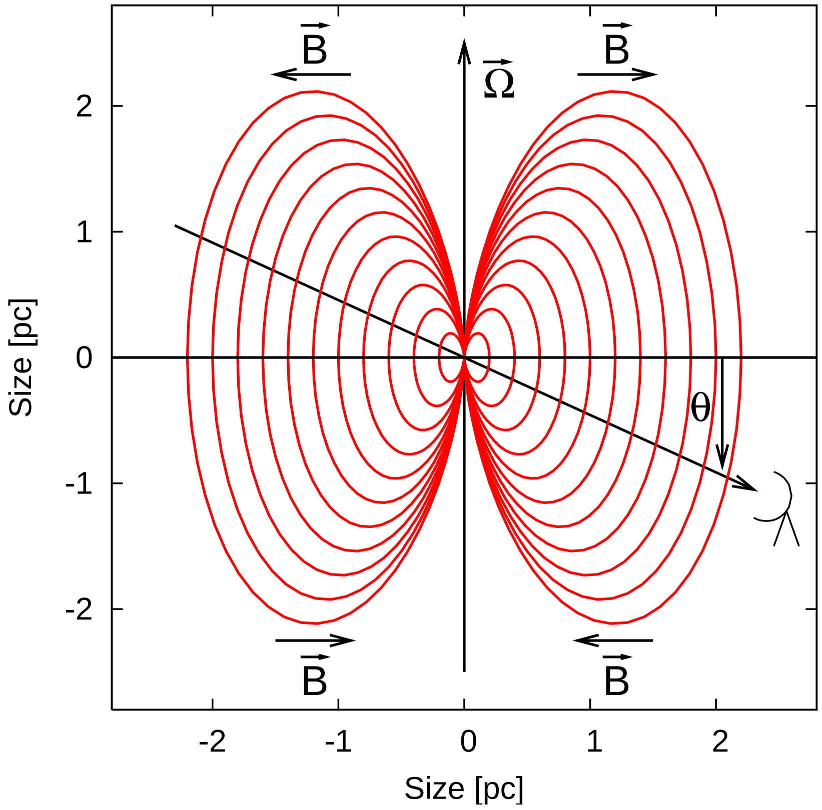

- Assuming that a dipole field is responsible for the Faraday rotation inside DA 495 we fitted this model to the RM map.
- We derive a magnetic field of 1.3 mG and an electron density of 0.3 cm^{-3} inside the nebula.

Kothes, Landecker, Reich, Safi-Harb, & Arzoumanian, 2008, ApJ 687, 516

DA 495

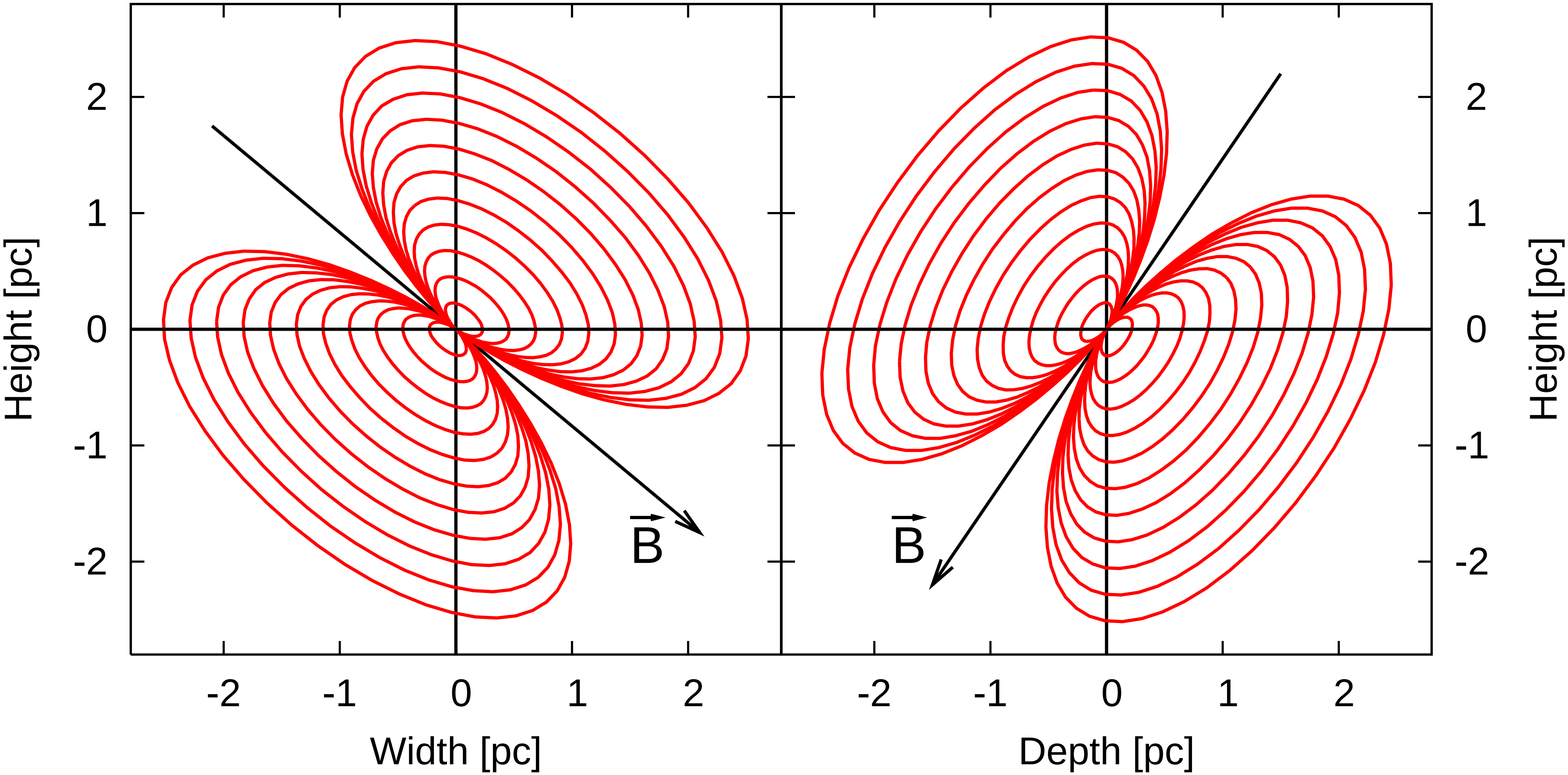

Kothes, Landecker, Reich, Safi-Harb, & Arzoumanian, 2008, ApJ 687, 516